Semiannual Progress Report

Submitted to:	National Aeronautics and Space Adminstration Langley Research Center Hampton, Va 23665
Institution:	Hampton University Dept of Physics and Engineering
Title of Research:	Direct Solar-Pumped Iodine Laser Amplifier
NASA Grant Number	NAG-1-441
Period Covered	Oct 1, 1985 - March 30, 1986
Principal Investigator	Dr. Kwang S. Han

(NASA-CR-177238) DIRECT SOLAR-PUMPED IODINE LASER AMPLIFIER Semiannual Progress Report, 1 Oct. 1985-30 Mar. 1986 (Hampton Inst.) 61 p HC A04/MF A01 CSCL 20E

N86-28399

Unclas G3/36 43393

Direct Solar-Pumped Iodine Laser Amplifier

Contents

I. Abstract i

II. A 10W CW Iodine Laser pumped by a Vortek Solar Simulator 1

A. Introduction 1
B. Experiment 2
C. Results 6
D. Summary 10
E. References 12
F. Caption of Figures 13

III. Kinetic Modeling of the Solar-Pumped Iodine Laser

A. Introduction 21
B. Average Photodissociation Rate 22
C. Heat Transfer 24
D. Discussion 27
E. Tables 28
F. Figures 33

IV. Parametric studies of Dye Laser Amplifier by Tamarack Solar Simulator

A. Introduction 42
B. Dye Laser Oscillator-amplifier System 45
C. Fluorescence Measurement 46
D. Amplifier Gain Measuremnt 47
E. Amplifier Gain Measurement as a Function of the Injection Time 47
F. References 48
G. Figures 49

I. Abstract

#13231

~~This semiannual progress report covers the period from Oct 1, 1985 to March 31, 1985 under NASA grant NAG-1-441 entitled "Direct solar-pumped iodine laser amplifier".~~ During this period the parametric studies of the iodine laser oscillator pumped by a Vortek simulator ~~has been~~ was carried out before amplifier studies. The amplifier studies are postponed to the extended period after completing the parametric studies. In addition, the kinetic modeling of a solar-pumped iodine laser amplifier, and the experimental work for a solar pumped dye laser amplifier are in progress. This report contains three parts: (1) A 10 W CW iodine laser pumped by a Vertek solar simulator, (2) kinetic modeling to predict the time to lasing threshold, lasing time, and energy output of solar-pumped iodine laser, and (3) the study of the dye laser amplifier pumped by a Tamarack solar simulator.

A. INTRODUCTION

Direct solar pumped lasers for use in space communications and power transmissions have been discussed since 1966.[1-3] The direct conversion of solar energy into coherent light is especially desirable because the construction of a huge and efficient solar energy collector is possible. The first attempt at solar pumped Nd-YAG laser using a 61 cm diameter f/1.5 aluminized paraboloidal mirror was reported by C. G. Young and obtained a laser output 1W during 7 ms.[1] Following Nd-YAG laser studies, the oscillation of an iodine photodissociation laser, a possible high power laser, was achieved. Using Xe-arc solar simulator a peak laser output of 4 W over 10 ms was obtained by J. H. Lee et al. in 1981.[4] A cw 18 W Nd-YAG laser using a 10 m diameter f/3.1 paraboloidal mirror was reported by H. Arashi et al. in 1984.[5]

Among the laser materials available at present time, the iodides such as C_3F_7I or C_4F_9I have advantages of broadband absorption of solar radiation and a low threshold. The atomic iodine photodissociation lasers first discovered in 1964[6] have been developed as a high power pulsed laser.[7,8] Recently a cw oscillation of atomic iodine laser was developed by L. A. Schlie in 1984 and a peak cw power of 38 mW was obtained using a DC Hg arc lamp by employing a closed cycle flow system for the laser material C_3F_7I.[9]

The cw iodine photodissociation laser provides the flow of laser material because of the irreversible consumption of the reactants produced by photolysis.[10]In this article we are reporting

the successful operation of a cw atomic iodine laser pumped by a vortex-stabilized solar simulator by employing a thermally driven blow-down system. It has virtually unlimited lifetime. A maximum cw power of 11 W laser was achieved by employing a blow-down flow system for the laser material n-C_3F_7I and operated over one hour.

B. EXPERIMENTS

B-1 Measurement of spectral irradiance of solar simulator

In this experiment the Vortek arc lamp was used as a pumping source of the photodissociation iodine laser. The optical radiation was produced in the lamp by a high pressure DC argon arc, which is vortex-stabilized and deionized water cooled. The arc is contained in a single quartz tube (Germasil grade) of 2.1 cm in diameter and 25 cm long with replaceable water-cooled tungsten electrodes at each end.Rapidly swirling deionized water inside of this tube efficiently removes the excess heat and prevents the deposition of electrode material. The maximum electrical input power is 100 kW and the optical radiative output is 45 kW. The arc size is 1.1 cm in diameter and 20 cm long and its emission is in the spectral range of 200 nm to 1400 nm. In order to measure the spectral irradiance in the spectral range of 200 nm to 400nm, a deutrium irradiance standard lamp (Optronics, model 45)was used to calibrate the spectrometer and the detector. In measurements wherein two sources (standard and Vortek arc lamp) were being

compared by the direct substitution method (slitwidths kept unchanged, use of the same detector), thus neither knowledge of the spectral transmittance of the spectrometer, nor knowledge of the spectral sensitivity of the detector was required.

The spectral irradiance of Vortek arc lamp on the laser tube was measured using the optical multichannel analyzer. The lights radiated from the simulator lamp were reflected by an elliptical cylindrical reflector and focused on the laser tube. To compensate for the different geometries of illumination between the Vortek arc lamp and the standard lamp, the grounded quartz tube (Superasil grade) was used as a diffuser. The deflected beam by a 45° mirror inside the grounded tube was collected by a quartz lens L and focused onto the spectrometer M as shown in Fig. 1. The spectral irradiance of Vortek arc lamp is compared directly with that of the calibrated deutrium lamp by rotating the 45° mirror towards deutrium lamp. The elliptical cylindrical reflector was taken off from the system, when measuring the irradiance of standard deutrium lamp. Since the irradiance of Vortek arc lamp was too high, the neutral density filter whose spectral density was known was used to reduce the intensity.

Fig. 2 shows the typical spectral irradiance of Vortek solar simulator with scaled-up air-mass-zero(AMO) solar spectrum in the wavelength region of 200 nm to 400 nm in which the absorption band of $n\text{-}C_3F_7I$ is located. The measured irradiance of simulator was 1250 times of AMO solar irradiance when the applied current on the Vortek arc lamp was 300 A. According to the previous result[11], the spectral irradiance of simulator was proportional to the square

of the current through the arc lamp. Actually the irradiance in Fig. 2 was calculated from the measured irradiance at 110 A by using the previous result. Also Fig. 2 shows that the simulator produces more uv radiation than AMO solar irradiance in the absorption band of n-C_3F_7I.

B-2 Operation of a cw iodine laser

A cw laser at 1.315 um was produced by the photodissociation of n-C_3F_7I flowing through a suprasil grade quartz tube.To transfer the uv radiation from a vortex-stabilized solar simulator lamp into the laser tube, both the arc lamp and the laser tube were placed at the focal line of an elliptical cylindrical reflector and two plate reflectors were placed at both ends of elliptical reflector. All surfaces were polished and coated with aluminum. The major axis of the elliptical reflector and the distance between foci are 35.5 cm and 17.8 cm respectively. The elliptical and two plane reflectors were water-cooled to remove the heat generated by the arc lamp. The laser tube was enclosed in a water-cooled suprasil quartz coaxial jacket through which the deionized water flowed. Two different sizes of suprasil laser tubes were used seperately and their inner diameters were 12mm and 16mm and their length was 45 cm. Only 15 cm of the tube was enclosed in the elliptical reflector, another 10 cm was in downstream of the optical pumping and the other 20 cm was in upstream to provide a uniform flow in the pumping region. At the both ends of the laser tube were mounted Brewster quartz window housings.

For lasing resonators of different type were employed. Resonator was consisted of 10 m in radius of curvature of mirrors, one totally reflecting mirror and output coupling mirror having reflectivity of 98%, 96%, 90%, 85%, 80%, or 70%. The distance between two mirrors was 0.85 m. To measure the laser output signal, two kinds of detectors were used, a fast responce germanium detector for detailed signal in time and a thermal disc powermeter(Coherent P-201) for the average power.

The n-C_3F_7I laser material was flowed to remove the I_2 molecules produced by the photolysis, since the I_2 is a strong quenching species of excited atomic iodine.[12] The n-C_3F_7I is a liquid in the room temperature and has a high vapor pressure (61.3 kPa at 300 K).[13] The flow of n-C_3F_7I was provided by the blow-down system. Before the laser operation the bottle containing iodides (n-C_3F_7I) was immersed in the liquid nitrogen dewar and pumped with a diffusion pump to remove air impurities. After degasing, the bottle was immersed in an alcohol dewar in the room temperature to prevent the temperature variation during the vaporization and stirred with a magnetic stirrer to help vaporization. On the other side of the laser tube the condensing bottle which was immersed in liquid nitrogen was connected. To measure the flow rate of iodides, the mass flowmeter(Hasting AHL-2G) which was calibrated for C F I was connected between the laser tube and the vaporization bottle. The flow rate was controlled by the valve on the line between the flowmeter and vaporization bottle. The flow velocity was measured from the pressures at

both sides of laser tube and the mass flow rate as shown in Fig.3.

After laser operation the iodide was distilled for the reuse at the next operation. This procedure was done mainly to remove the I_2 produced after photolysis. The condensation bottle was warmed up to the room temperature after a laser action and was connected to another evacuated bottle through the filter containing copper wire mashes. This filter was kept below a temperature of -10°C during the distillation process and experienced need of a slow flow of the iodide chemical for a better distillation process. After distilling the iodide this bottle was replaced by an empty vaporization bottle and then reused at the next laser operation.

The laser tube, the condensing bottle and the distillation system were evacuated by a diffusion pump with liquid nitrogen trap and checked the leaks in the vacuum system. If the leakrate is significantly large, the O_2 and N_2 impurities quench the excited atomic iodine. Therefore the experiment was done when the leakrate was less than 0.1Pa during 5 minutes. With this system the laser was operated over one hour with 1 kg of $n\text{-}C_3F_7I$ at the low flow rate (140 sccm).

C. RESULTS

The laser output signal and the light signal of Vortek simulator were measured simultaneously by using a germanium photovoltaic detector and a silicon photodiode respectively. The laser excitation was continuously observed over one hour without any break.

The periodic variation of the laser output signal shown in Fig. 4 was due to the ripple of the electrical input power of the solar simulator as appeared in the light signal in Fig. 4. The ripple frequency was 360 Hz which is exactly the same as the frequency of three phase rectifier circuit. The reason of the spiking signal appeared in the laser output was not identified yet. But the laser signal has DC offset which shows the laser operation in truely continuous wave. The average output power which measured with a thermal disk power meter was 0.2 W when the laser tube of 12 mm i.d. and 2% transmitting mirror as a coupler were used. The flow rate of $n\text{-}C_3F_7I$ was 1740 sccm.

To find the optimum cavity condition, the coupling mirrors with various transmissions were used. The optimum transmission of the output coupling mirror was 15% when the applied current and the flowrate were 200 A and 1740 sccm respectively. Under this condition the maximum output power was 1.3 W.

Fig. 5 shows the laser output power versus the flow rate of $n\text{-}C_3F_7I$ for different sizes of laser tube at the optimum cavity condition. The pressures at the both ends of laser tube were linearly proportional to the flow rate of $n\text{-}C_3F_7I$. This means that the velocity of the iodide molecules in the laser tube remained constant for different flow rate. The average velocity of the iodide molecule in the laser tube was 18 m/s when a 12mm i.d. tube was used. The dwell time which the iodide molecule passes the illumination region (15 cm) was 8.3 ms. When a 16 mm i.d. tube was used, the velocity and the dwell time were 12 m/s and 12.5 ms respectively. The laser output power was increased when the flow

rate was increased and the increasing ratio was slow down at higher flow rate. As shown in Fig. 5 the power was increased about 40% when the larger tube was used. But the ratio was not proportional directly to the cross-sectional area of the tubes. When the current increased to 280 A, the output power was increased about 60%.

Fig. 6 shows the laser output power dependent on the electrical input power applied to Vortek arc lamp. When the flow rate was fixed, the laser output power was proportional to the electrical input power. The slope efficiency for the electrical input power applied to the arc lamp was 0.013%. When the 16 mm i.d. tube was used and the flow rate was 2300 sccm, the threshold electrical input power was approximately 10 kW which corresponds to 90 solar concentrations. The internal laser efficiency corresponding to the irradiance into the laser tube was 0.085%. When the flow rate was increased to 3500 sccm, the laser output power was increased upto 10.5 W at applied current of 300 A.

The laser beam profile was measured by using a IR sensitive video camera through the laser output coupling mirror as shown in Fig. 7. The laser beam diameter at the coupling mirror was approximately 7 mm and had almost a square top shape. With mirrors of 10 m and a mirror seperation of 0.8 m, the laser beam diameter at the output coupling mirror would be 2 mm if the TEM_{OO} mode was assumed. It was found that the laser oscillated as multimodes, not a TEM_{OO} mode with this measurement.

Finally the temperature of the gas after passing the laser tube was measured with a thermocouple junction. Two thermocouple junctions were placed, one on the outside wall of a stainless tube connected on the laser tube through the Brewster window housing and the other in the center of the tube to measure the gas temperature. The flow rate of iodides and the applied current on the arc lamp were kept as constants and were 2900 sccm and 300 A(maximum operational current) respectively. When the simulator was turned on, the temperatures were raised very slowly because of a direct exposure of leaked radiation from the system.When the flow of iodides started, the temperature of the gas inside the tube jumped up rapidly to 100°C from a room temperature. The gas temperature was raised upto 150°C after 10 minutes operation and then stabilized. This result is important for the design of a solar pumped laser in space. When the pumping intensity was equivalent to 1270 solar concentrations and the flow rate was 2900 sccm, the gas temperature was raised upto 150°C. If the flow system in the space baced laser is driven thermally, the gas temperature and the thermal conductivity of iodides should be considered in the flow system design. Another effect is the energy storage time in the amplifier system for high power laser. As the gas temperature rose, the storage time was shortened in the amplifier system.[14] But if the solar concentration system such as a parabolic trough is used, the limit of the concentration is low (150 times). The effects of elevating temperature will be eliminated by using such a low concentrating system.

0. SUMMARY

A cw iodine photodissociation laser pumped by a solar simulator was obtained over one hour and the maximum cw output power was 10W with a 16 mm i.d. laser tube and thermally driven blowdown flow system. With this system the threshold pumping was 90 solar concentrations. The output beam profile and the gas temperature was measured. These results indicate that the solar pumped iodine cw laser can be scaled up to a high power level that is significant for space applications.

E. REFERENCES

1. C. G. Young, Applied Optics 5, 993-997(1966).
2. M. Ross, P. Freedman, J. Abernathy, G. Matassov, J. Wolf and J. D. Barry, Proc. IEEE 66, 319-344(1978).
3. A. L. Golger and I. I. Klimovsky, Proc. International conference on Lasers '83, 686-693(1983).
4. J. H. Lee and W. R. Weaver, Appl. Phys. Lett. 39,137-139(1981).
5. H. Arashi, Y. Oka, N. Sasahara, A. Kaimai and M. Ishigame, Japanese J. Appl. Phys. 23, 1051-1053(1984).
6. J. V. V. Kasper and G. C. Pimental, Appl. Phys. Lett. 5, 231 (1964).
7. G. Brederlow, K. J. Witte, E. Fill, K. Hohla and R. Volk, IEEE J. Quant. Electron. QE-12, 152-155(1976).
8. H. J. Baker and T. A. King, Jounal De Physique 41, C9-359-362(1980).
9. L. A. Schlie and R. D. Rathge, IEEE J. Quant. Electron. QE-20, 1187-1196(1984).
10. R. W. F. Gross and J. F. Bott, "Handbook of Chemical Lasers", Chapter 12, John Wiley and Sons, New York (1976).
11. K. S. Han, Semiannual Progress Report, NAG-1-441(1985).
12. J. J. Deakin and D. Husain, Chemical Soc. Faraday II 68,1603-1612(1972).
13. W. Fuss and K. Hohla, Opt. Commun. 18, 427-430(1976).
14. I. H. Hwang, J. H. Lee and M. H. Lee, Opt. Commun. Will be published.

FIGURES

1. Experimental setup for solar irradiance measurement of Vortek solar simulator. L ; collecting lens, ND ; neutral density filter, M ; spectrometer, OMA ; optical multichannel analyzer.
2. Spectral irradiance of Vortek solar simulator on laser tube with solar irradiance and absorption coeffecient of $n\text{-}C_3F_7I$. Applied current on simulator was 300 A.
3. Experimental setup for a cw iodine laser pumped by Vortek solar simulator. F ;mass flow meter, P_i, p_o; pressure gauge, D; detector.
4. Laser output signal with pumping light signal from solar simulator.
5. Laser output power for different flow rate of $n\text{-}C_3F_7I$.
6. Laser output power for the electrical input power of solar simulator.
7. Laser beam profile photographs taken at the coupling mirror by IR video camera.
8. Measured gas temperature in the laser tube. Flow rate; 2900 sccm, applied current of solar simulator ; 300 A.

MEASUREMENT OF SPECTRAL IRRADIANCE

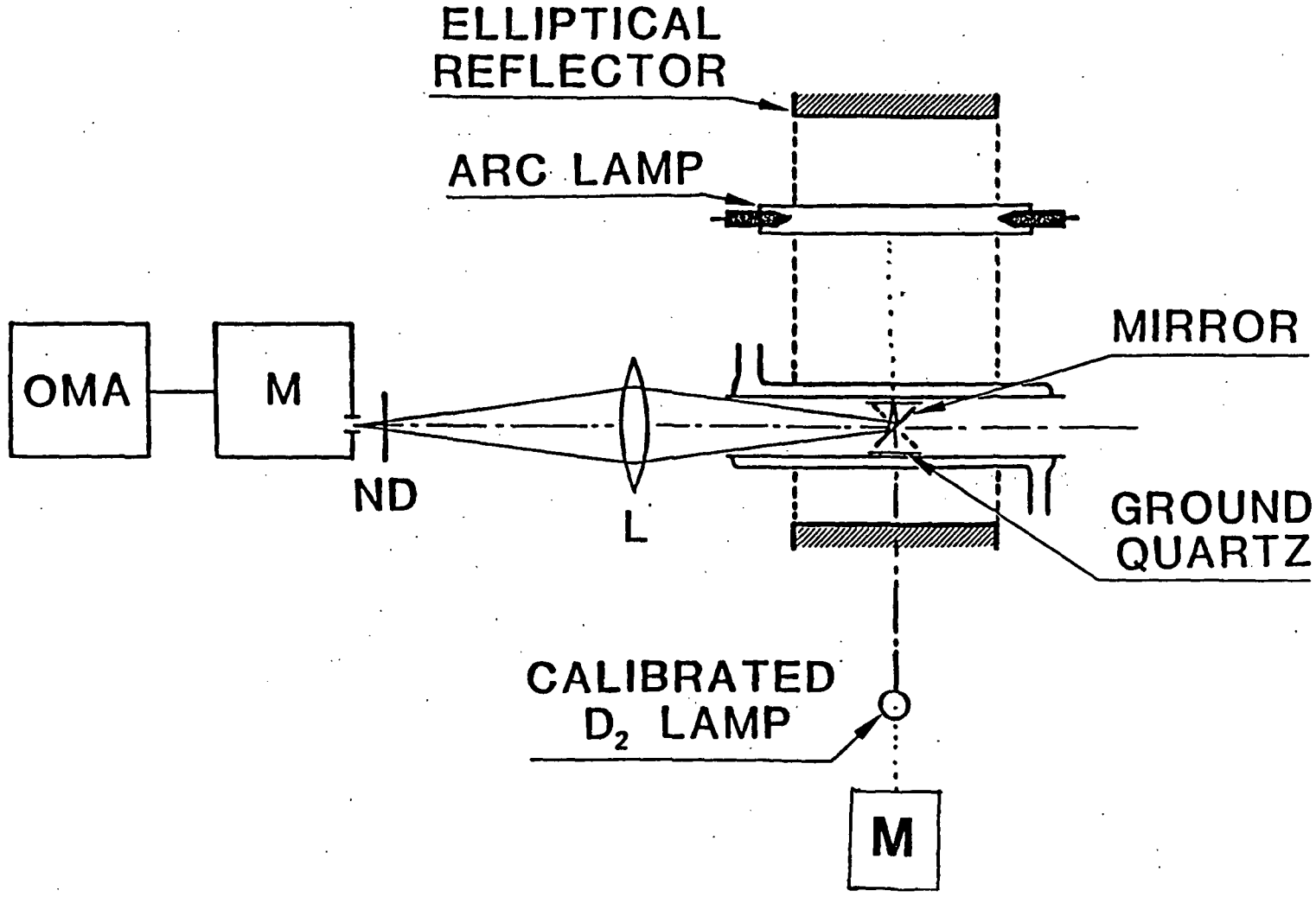

Fig. 1 Experimental setup for solar irradiance measurement of Vortek solar simulator. L; collecting lens, ND; neutral density filter, M; spectrometer, OMA; optical multichannel analyzer.

Fig. 2 Spectral irradiance of Vortek solar simulator on laser tube with solar irradiance and absorption coefficient of n-C_3F_7I. Applied current on simulator was 300 A.

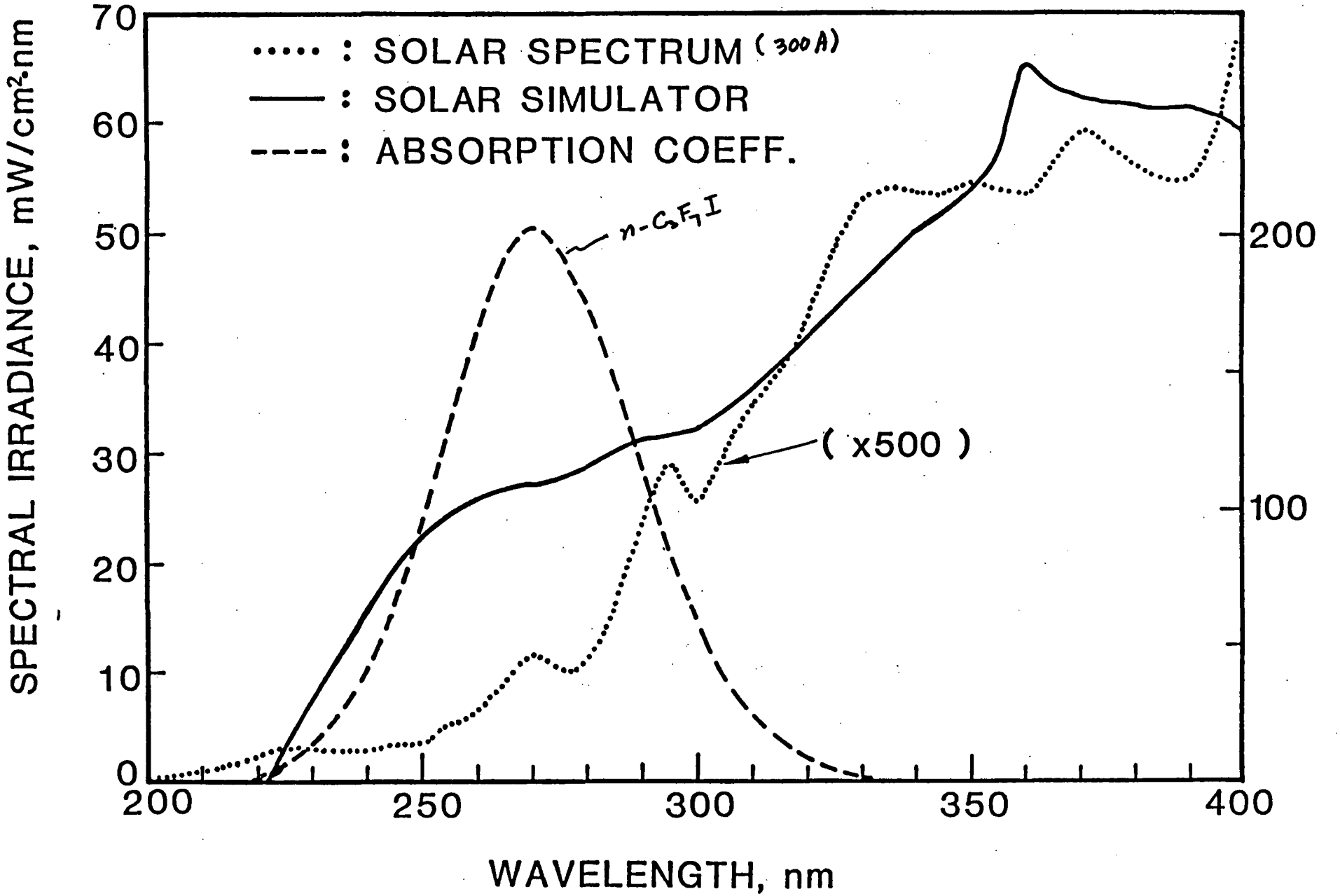

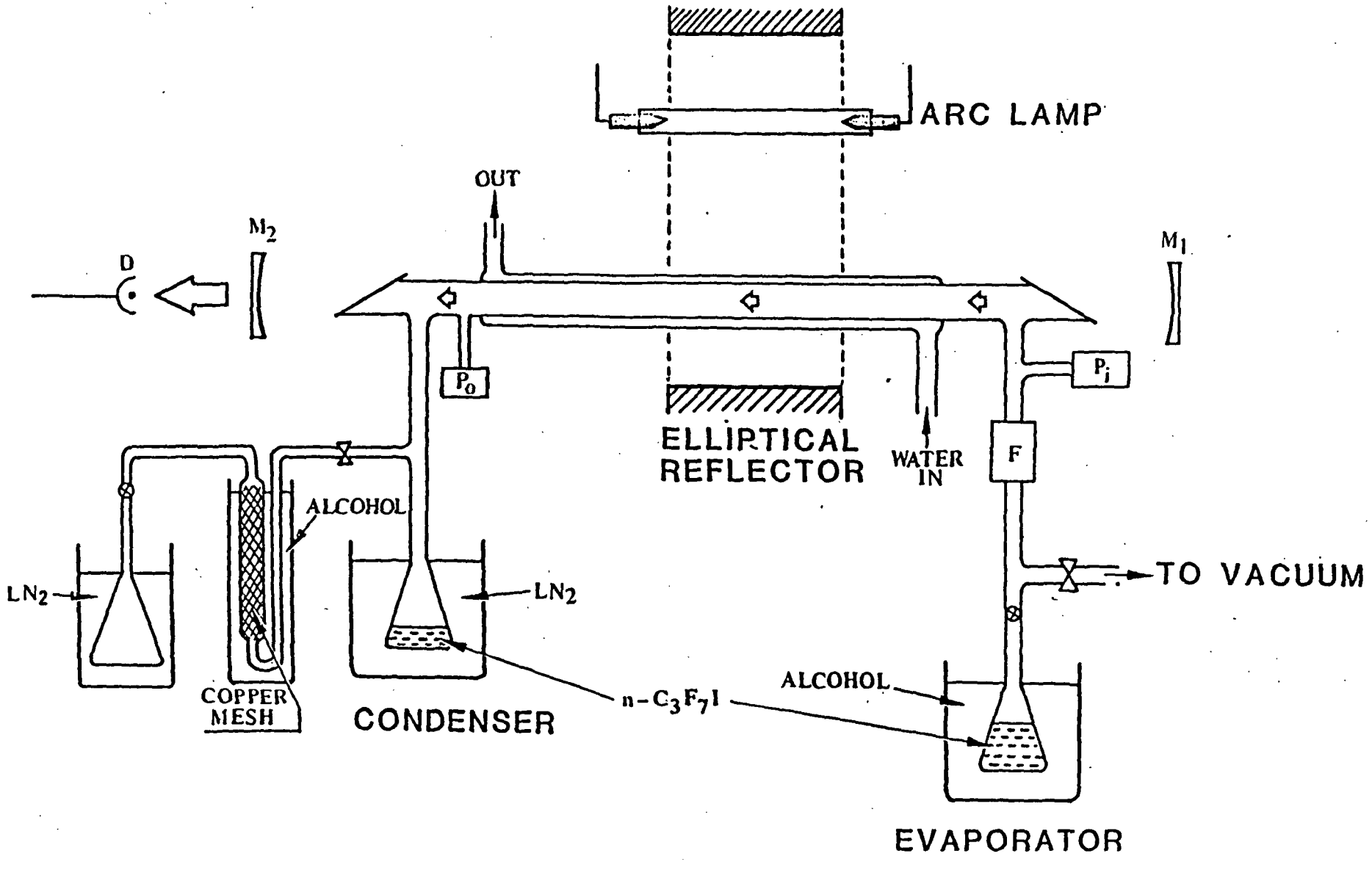

Fig. 3 Experimental setup for a cw iodine laser pumped by Vortek solar simulator. F; mass flow meter, P_i, P_o; pressure gauge, D; detector.

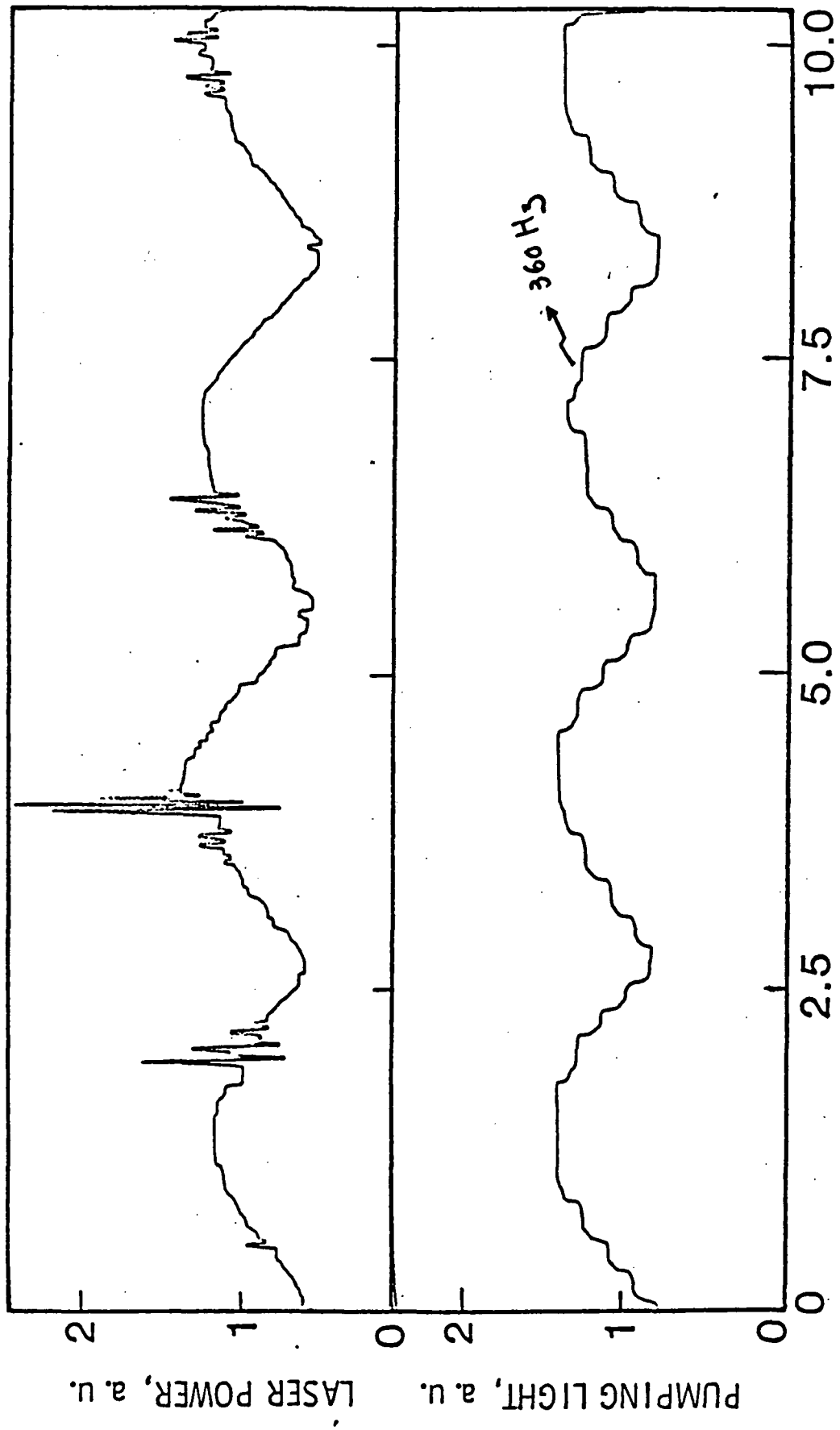

Fig. 4 Laser output signal with pumping light signal from solar simulator.

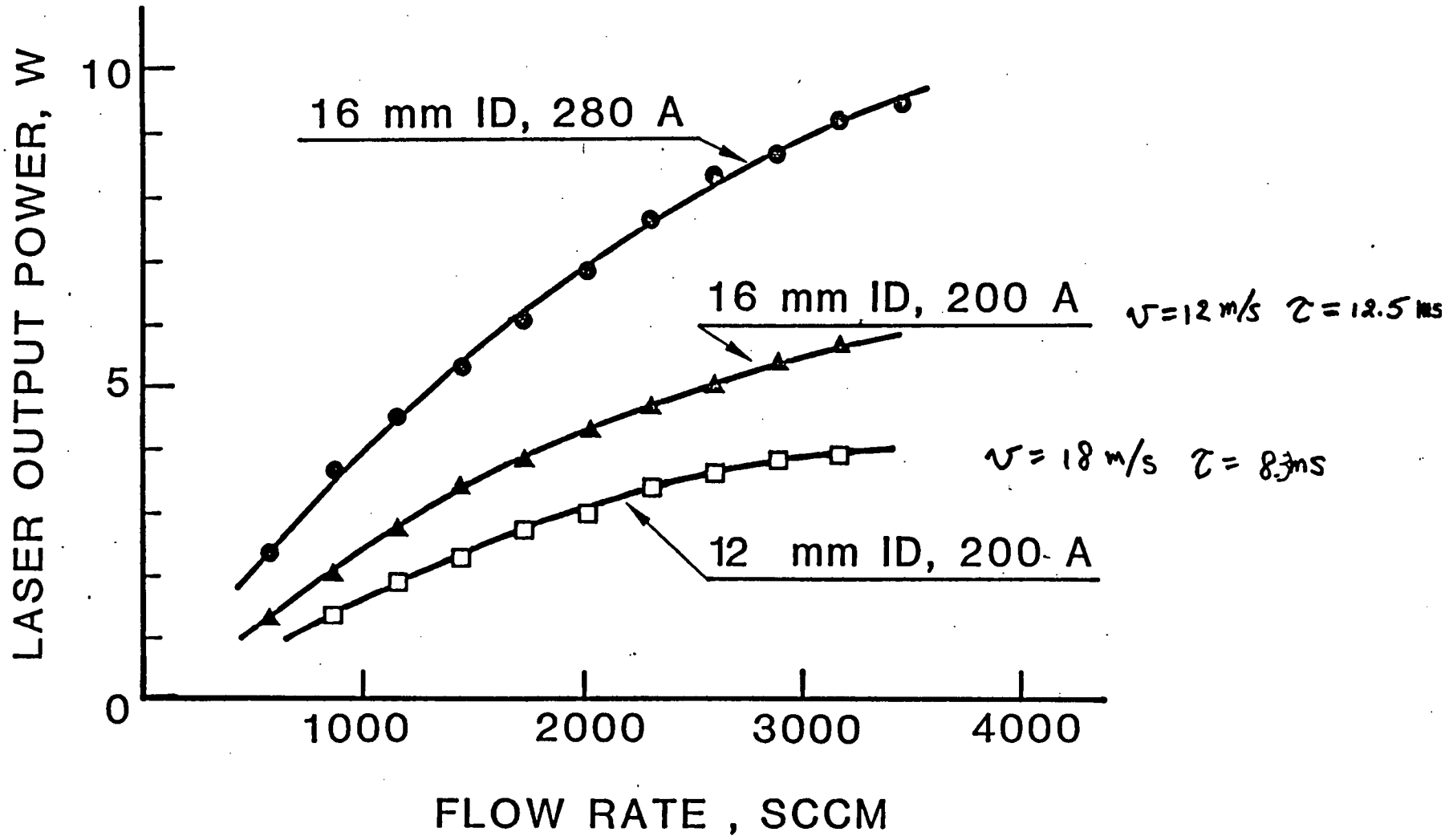

Fig. 5 Laser output power for different flow rate of n-C_3F_7I.

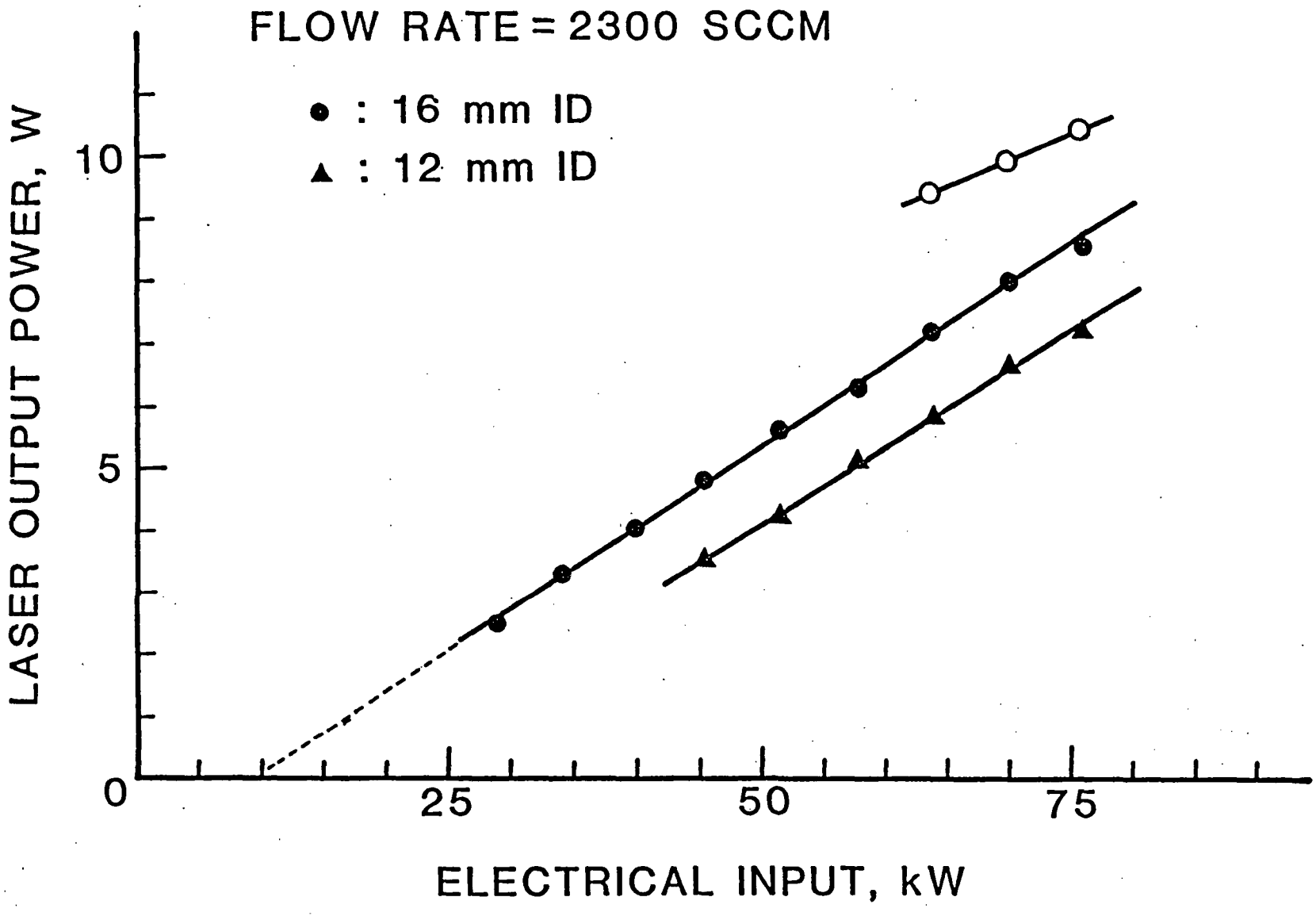

Fig. 6 Laser output power for the electrical input power of solar simulator.

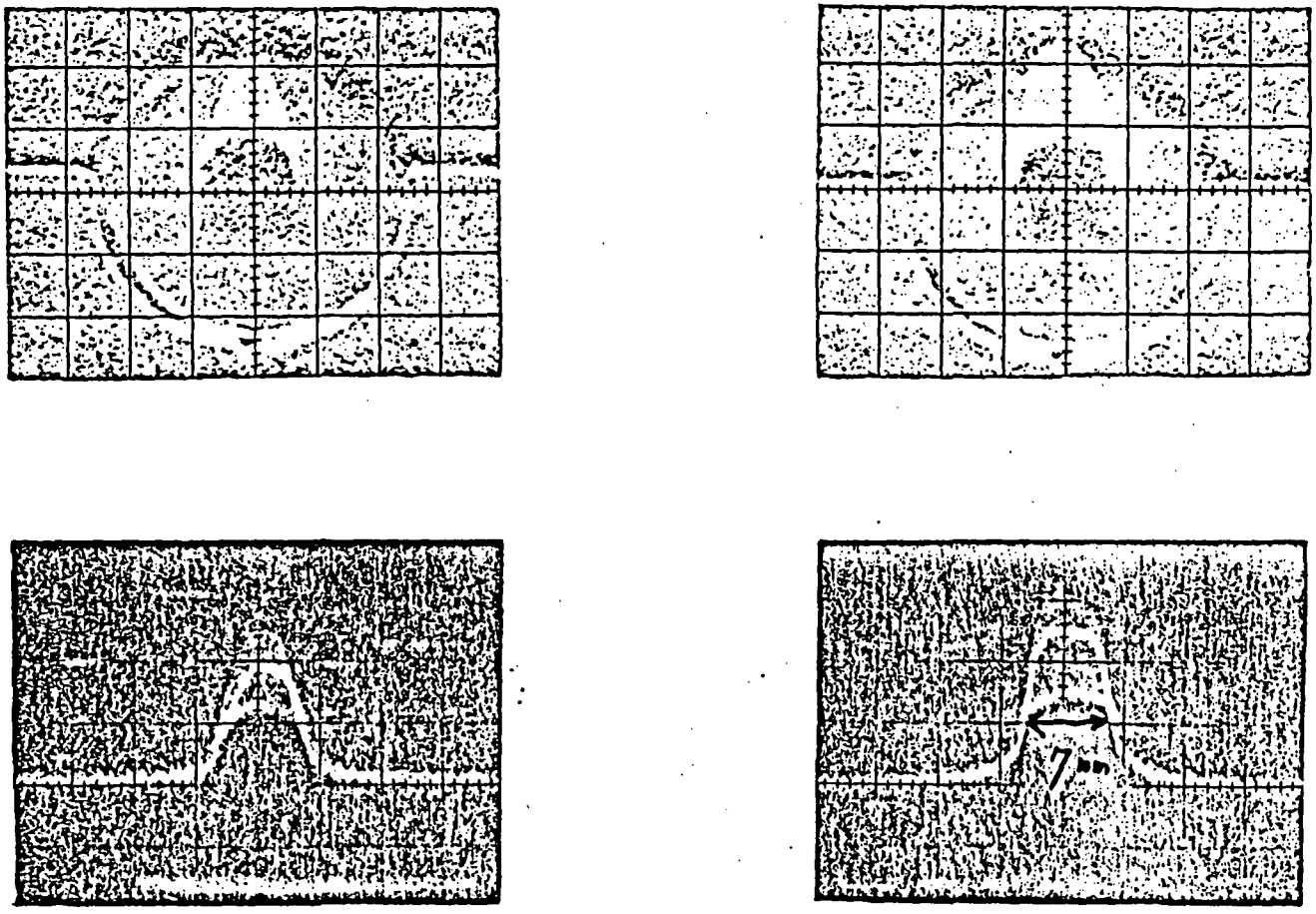

Fig. 7 Laser beam profile photographs taken at the coupling mirror by IR video camera.

Fig. 8 Measured gas temperature in the laser tube. Flow rate; 2900sccm, applied current of solar simulator; 300A.

Flow : 2880 sccm
Current : 300 A

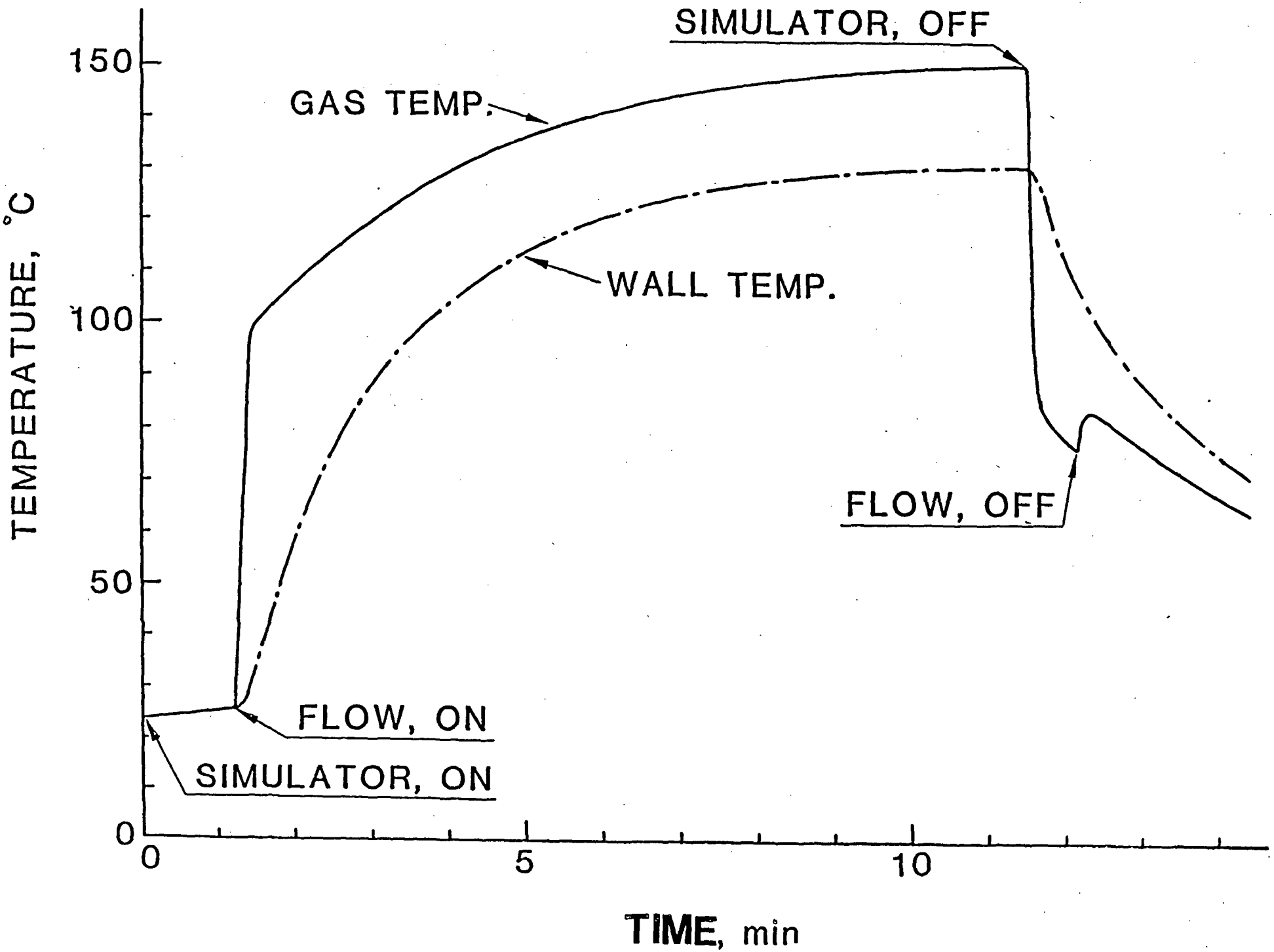

III. Kinetic Modeling of Solar-Pumped Iodine Laser

A. Introduction

This report relates the work performed from September 1, 1985, to April 30, 1986. During this period the modeling project to predict the time to lasing threshold, lasing time, and energy output of solar-pumped iodine lasers has progressed. Thereby analyzing the effects of the different physical experimental parameters and the lasant's gas kinetics on the above output parameters. To this end, a computer model is being developed which will fit the experimental data for the flashlamp pumped iodine laser oscillator system and a long path length solar-pumped laser, with turning mirrors inside a rectangular resonator cavity.

By adjusting the reaction rate coefficients within known experimental bounds the output parameters for the two lasing systems are predicted, thereby giving important information about the affect the different kinetic reactions have upon these same output parameters. The adjustment of the kinetic coefficients is accomplished by numerical methods. The information gained about the kinetics in the lasant can be used to model other iodine gas lasers; amplifiers, continuous pulse lasers, etc. In addition, the modeling process can be used to maximize output parameters of a laser system by adjusting the physical makeup of the lasing system. For instance, the pressure may be adjusted to find the maximum energy output.

To this date, the development of the model for the flashlamp pumped iodine laser oscillator system has included the average photodissociation

rates ξ_i of the laser tube for the three different solar-pumped media, i-C_3F_7I, n-C_4F_9I, and t-C_4F_9I; a function for the input pulse; a temperature model for the lasant gas; and the conversion of the kinetic model with associated fitting routines to give the preliminary results shown in figures 1 and 2. In addition, the work for the long-path laser experiment using i-C_3F_7I as a lasant has further progressed to include a delineation of the bounds for the kinetic coefficients (table 1), a new model for the heat of the cavity gas, and a new fit shown in figures 3, 4, and 5. The new fit to the experimental data by the kinetic model is promulgated by the new temperature derivation and allowing the kinetic coefficient K_3 ($9.0 \times 10^{-13} \times 3.8 \pm 1$ cm^3/sec) to go beyond the upper bound found experimentally for the reaction $R + R \rightarrow R_2$.

B. Average Photodissociation Rate

In order to find the average photodissociation rate the arc lamp image must be coupled to the gas in the tube cavity. Ideally, the image of the arc lamp is located at the laser tube since the laser tube and the arc lamp are at the two focii of an elliptical reflector. In order to couple the laser tube to the lamp the reflectances $R(\lambda)$ of the aluminum surface (table 2) of the elliptical reflector must be taken into account. In addition, since there may be variations in the intensity $I(\theta)$ at the tube from the arc lamp as a function of angle (fig. 6), these intensities must be averaged over that θ. Therefore, including a coupling factor for the aluminum elliptical reflector, the photodissociation rate becomes

$$S_i = \frac{\int I(\theta)d\theta \int_0^\infty \phi(\lambda)\,\sigma(\lambda)\,R(\lambda)\,d\lambda}{I_0 R(\lambda_{vis}) \int d\theta}$$

where I_0 is the reference intensity from the arc lamp for which the $I(\theta)$ measurements are taken, λ_{vis} (520 nm) is the wavelength that the intensity measurements were taken (table 2), and $\phi(\lambda)$ is the flux density found experimentally (fig. 7). The photoabsorption cross section is given by

$$\sigma(a) = \sigma_0 \exp\left[\frac{-(\lambda - \lambda_0)^2}{4\delta_0^2}\right]$$

where the peak cross section σ_0, line center λ_0, and line width δ_0 is given in table 3, for different gases as measured previously. The integration is done numerically using Gauss-Hermite quadratures.

The relative attenuation of the light at a given distance x and fill pressure p_0 is given by

$$f(x,p_0) = \left[f \exp(-n\sigma_0 x) + (1 - f) \exp(-0.223\ n\sigma_0 x)\right]$$

where the lasant gas density n is given by $3.2 \times 10^{16}\ p_0$. Since the total output energy was measured, an average attenuation must be used which is found by

$$F(p_0) = \int_0^{r_w} x\ f(x,\ p_0)\ dx \Big/ \int_0^{r_w} x\ dx$$

where r_w is the inside radius of the laser tube (.35 cm). Therefore, the rate I* is formed inside the laser tube for the ith gas is given by

$$\xi_i = \Phi_{I*}\ F(p_0)\ S\ I(t)\ n$$

where the iodides and I_2 photodissociate into fractions Φ_{I*} of metastable iodine with values of 100 percent and 51 percent, respectively (see table 3). I(t) is the intensity of the arc lamp as a function of time for the UV light and the visible light (fig. 8).

$$I_{UV}(t) = [2.071 + 647.703\{1-\exp[-2.1738(t + 35 \times 10^{-6})]\}$$

$$\{1-\exp[1.3968(t - 891 \times 10^{-6})]\}]/583.55$$

$$I_{vis}(t) = [.4843 + 1777.02\{1-\exp[1.7855(t + 30 \times 10^{-6})]\}$$

$$\{1-\exp[0.86085(t - 946 \times 10^{-6})]\}]/1439.4$$

where the peak is normalized to one and $I_{UV}(t)$ is used for the iodides and $I_{vis}(t)$ is used for the visible light intensity to calculate the photodissociation rate for I_2. The results of the calculation are given in table 4 for different fill pressures and gases for the peak intensity ($I(t) = 1$).

C. Heat Transfer

Within the model of the laser kinetics a heat transport calculation for the gas is made. A simple model of heat diffusion from the volume of the exposed gas to the wall is made. This model will give an approximate value for the raise in temperature which will, in turn, modify the pressure of the cavity gas.

Experimentally, after a laser pulse in this configuration, the tube's exterior temperature rises less than a couple of degrees. Therefore, it is first assumed that the temperature of the tube remains a constant. The heat diffusion equation is given as

$$\rho_g C_v \frac{\partial T}{\partial t} = k \nabla^2 T + q \quad ,$$

where $\rho_g C_v$ is the heat capacity per unit volume, k is the thermal conductivity, q the source of heat from photolysis. To approximate $k\nabla^2 T$

$$\rho_g C_v \frac{\partial \bar{T}}{\partial t} v = k \int_v \nabla \cdot \nabla T dv + \int_v q dv$$

which becomes

$$\rho_g C_v \frac{\partial \bar{T}}{\partial t} \frac{k}{L} [(\nabla T)_s] + q$$

where the heat capacity C_v is approximated as 40 cal/mol °C and $(\Delta T)_s$ is the temperature gradient at the inside surface of the tube. The average heat gain is given as

$$\bar{q} = \Delta E/\Delta V \, \Delta t$$

where the change in internal energy is given by

$$\Delta E = \epsilon_o \xi_1 dt + \epsilon_1 k_1 [I^*][R] \, dt +$$
$$\epsilon_2 k_2 [I][R] \, dt + \epsilon_3 k_3 [R][R] \, dt$$

where ϵ_i is the energy released to the medium for the respective reactions (NASA TP 2241, "Threshold Kinetics of a Solar-Simulator-Pumped Iodine Laser," J. W. Wilson, et al., Feb. 1984).

To approximate $(\nabla T)_s$ the steady state solution is found from

$$k \nabla^2 T + q = o$$

to be

$$T = T_w + \frac{r_w^2 q}{4k} \quad \frac{r^2 q}{4k}$$

such that

$$(\Delta T)_s = -r_w q/2k$$

is found from above. To find an effective convection coefficient h, from the steady state solution, it is known

$$h(T^w - T^m) = k(\Delta T)^s/r^w = -q/2$$

and if T_m is taken as the midpoint temperature

$$(T_w - T_m) = \frac{-3\ r_w^2 q}{16k}$$

which gives

$$h = \frac{16\ k}{3\ r_w^2}$$

after substituting above. Therefore, a time depend solution is found as

$$\frac{\partial T}{\partial t} = \frac{16}{3}\ \frac{k}{r_w^2 \rho_g C_v}\ (T_w - T) + \frac{q}{\rho_g C_v}$$

where ρ_g is the gas density [RI] and

$$\tau_c = \frac{3}{16}\ \frac{r_w^2 \rho_g C_v}{k}$$

a conduction time constant which is

$$\tau_c = 3/4\ \tau_D$$

where τ_D is the diffusion time constant found in NASA TP-2241 as approximately 8.5×10^{-4} sec/torr. Similarly, a heat conduction time constant τ'_c is found for the long path laser experiment to be

$$\tau'_c = 4/9\ \tau'_D$$

where τ'_D is the diffusion time constant for the rectangular cavity.

These values for the time constants are used in the kinetic models to predict the time to threshold, lasing times, and energy output for the two experiments discussed herein.

D. Discussion

A preliminary result for the pulse laser's fit to the time to lase threshold and output energy is shown in figures 1 and 2 for i-C_3F_7I. The kinetic reaction rates found from the long path solar pumped laser using i-C_3F_7I is used to find this fit. In order to get this result the physical dimensions of the laser's construction have been put in the kinetic model as described in TP-2241 and the output of the flashlamp has been coupled with the laser tube to get the photodissociation rate. A further experiment is to be performed to identify the internal losses of the laser tube.

After this experiment is performed the coupling of the flashlamp to the cavity will be concluded. This will enable us to fit the data given in table 5 for the time to lase threshold and the energy output. In addition, a fit of the laser pulse's power output will be accomplished. This should further identify the reactions and reaction rates in the lasant.

E.

Table 1.- Bounds for the Reaction Rate Coefficients defined by this experiment compared to previously reported results.

Bound defined by this experiment	Rate coefficient	Bound for previously published results
$1.7 \times 10^{-13}(17)^{-0.85}$	$\geq K_1$ $cm^3/s \geq$	$1.7 \times 10^{-13}(17)^{-1.0}$
$7.0 \times 10^{-17}(4.1)^{-.54}$	$\geq Q_1$ $cm^3/s \geq$	$7.0 \times 10^{-17}(4.1)^{-1.0}$
$3.9 \times 10^{-11}(4.3)^{0.84}$	$\geq K_2$ $cm^3/s \geq$	$3.9 \times 10^{-11}(4.3)^{1.0}$
$1.9 \times 10^{-11}(2.6)^{-0.97}$	$\geq Q_2$ $cm^3/s \geq$	$1.9 \times 10^{-11}(2.6)^{-1.0}$
$8.3 \times 10^{-32}(5.3)^{-0.99}$	$\geq C_2$ $cm^6/s \geq$	$8.3 \times 10^{-32}(5.3)^{-1.0}$

Table 2.- Reflectance $R(\lambda)$ of the reflector-collector in UV and visible ranges of spectrum.

Wavelength, nm	Reflectance, %
240	5.1
250	5.8
260	6.0
270	7.1
275	7.8
280	7.9
290	8.3
300	9.4
350	11.2
400	15.0
440	18.9

Table 3.- Photoabsorption Parameters Used

Parameter	$i\text{-}C_3F_7I$	$n\text{-}C_4F_9I$	$t\text{-}C_4F_9I$	I_2
σ_o, cm^2	6.2×10^{-19}	6.6×10^{-19}	4.8×10^{-19}	9.14×10^{-19}
λ_o, nm	275	273	290	499
δ_o, nm	14.5	12.66	15.18	23.0
Φ_I*	1.0	1.0	1.0	0.51
f	0.653	0.653	0.653	0.673

Table 4.- The rate at which I* is formed in the laser tube for different pressures and different gases for a gas density of 3.2×10^{17} molecules per cm^3.

p_o(torr)	$\xi_i \times 10^{21}$ (Number of photodissociations per second)			
Pressure	$i\text{-}C_3F_7I$	$n\text{-}C_4F_9I$	$t\text{-}C_4F_9I$	I_2
5	.402	.338	.334	1.35
10	.791	.663	.660	2.64
15	1.17	.977	.977	3.86
20	1.53	1.28	1.29	5.02
25	1.88	1.57	1.59	6.12
30	2.22	1.85	1.88	7.17
40	2.87	2.39	2.44	8.17

Table 5.- Experimental data found in the previously reported "Experiment on Perfluorobutyl Iodides as Solar-pumped Media for a Flashlamp Pumped Iodide Laser Oscillator System."

Lasant	Pressure (torr)	Pulse Energy (J/cm^2)	Threshold Time (μs)
$i\text{-}C_3F_7I$	5	0.0173	256
	10	0.0348	225
	15	0.0464	188
	20	0.0524	186
	25	0.0515	197
	30	0.0464	203
	40	0.0235	240
$n\text{-}C_4F_7I$	5	.0227	167
	10	.0459	155
	15	.0561	148
	20	.0697	137
	25	.0666	142
	30	.0547	155
	40	.0334	162
$t\text{-}C_4F_7I$	5	.0227	225
	10	.0481	215
	15	.0779	190
	20	.0929	195
	25	.103	210
	30	.101	217
	40	.0802	265

F. Figure Captions

Figure 1.- The pulse energy (J/cm^2) plotted as a function of pressure (torr) for i-C_3F_7I comparing the experimental data and the theoretical prediction (solid line) for the experiment on perfluorobutyl iodides as a solar-pumped media using the bounds given in table 1 for the rate coefficients.

Figure 2.- The threshold time (sec) plotted as a function of pressure (torr) for i-C_3F_7I comparing the experimental data and the theoretical prediction (solid line) for the experiment on perfluorobutyl iodides as a solar-pumped medi using the bounds given in table 1 for the rate coefficients.

Figure 3.- Results of kinetic model using rate coefficients given in table 1 for lasing times vs pressure for 85 percent and 97 percent reflectivities as compared to experimental data given by the solar-pumped laser with a rectangular resonator cavity.

Figure 4.- Results of kinetic model using rate coefficients given in table 1 for threshold times vs pressure for 85 percent and 97 percent reflectivities as compared to experimental data given by the solar-pumped laser with a rectangular resonator cavity.

Figure 5.- Results of kinetic model using rate coefficients given in table 1 and cut-off times given by experiment for pulse energy vs pressure for 85 percent and 97 percent reflectivities as compared to experimental data given by the solar-pumped laser with a rectangular resonator cavity.

Figure 6.- Variations of the fluences as a function of angle (θ).

Figure 7.- The fluence out of the flashlamp as a function wavelength. The experimental data ($\diamond$) and the corresponding sline (solid line) is plotted in addition to fluence given by 7000°K and a 6000°K blackbody radiator.

Figure 8.- The relative power out of the flashlamp given as a function of time (2 times μs) for the visible and UV wavelengths and their fits (solid line).

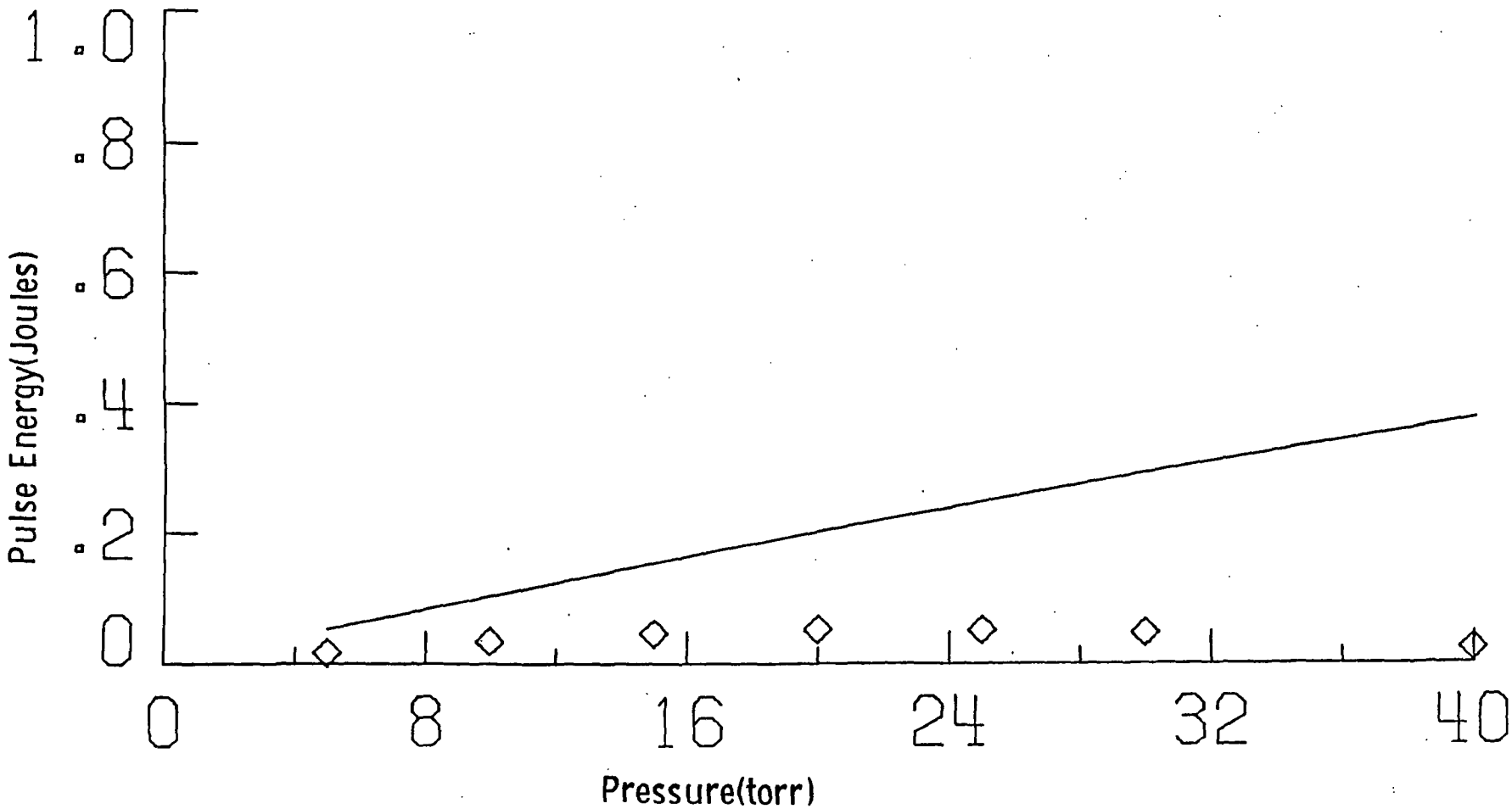

Figure I.

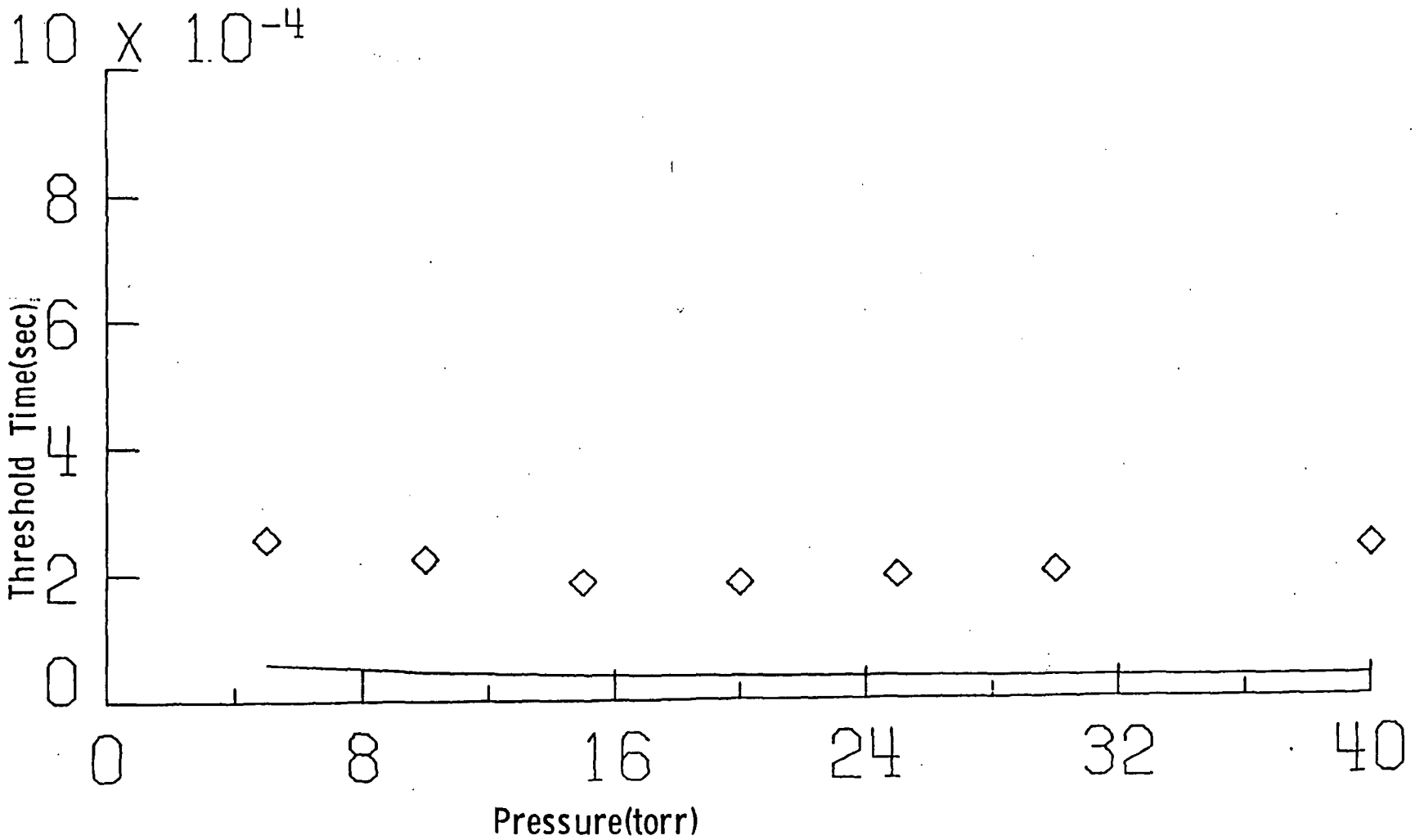

Figure 2.

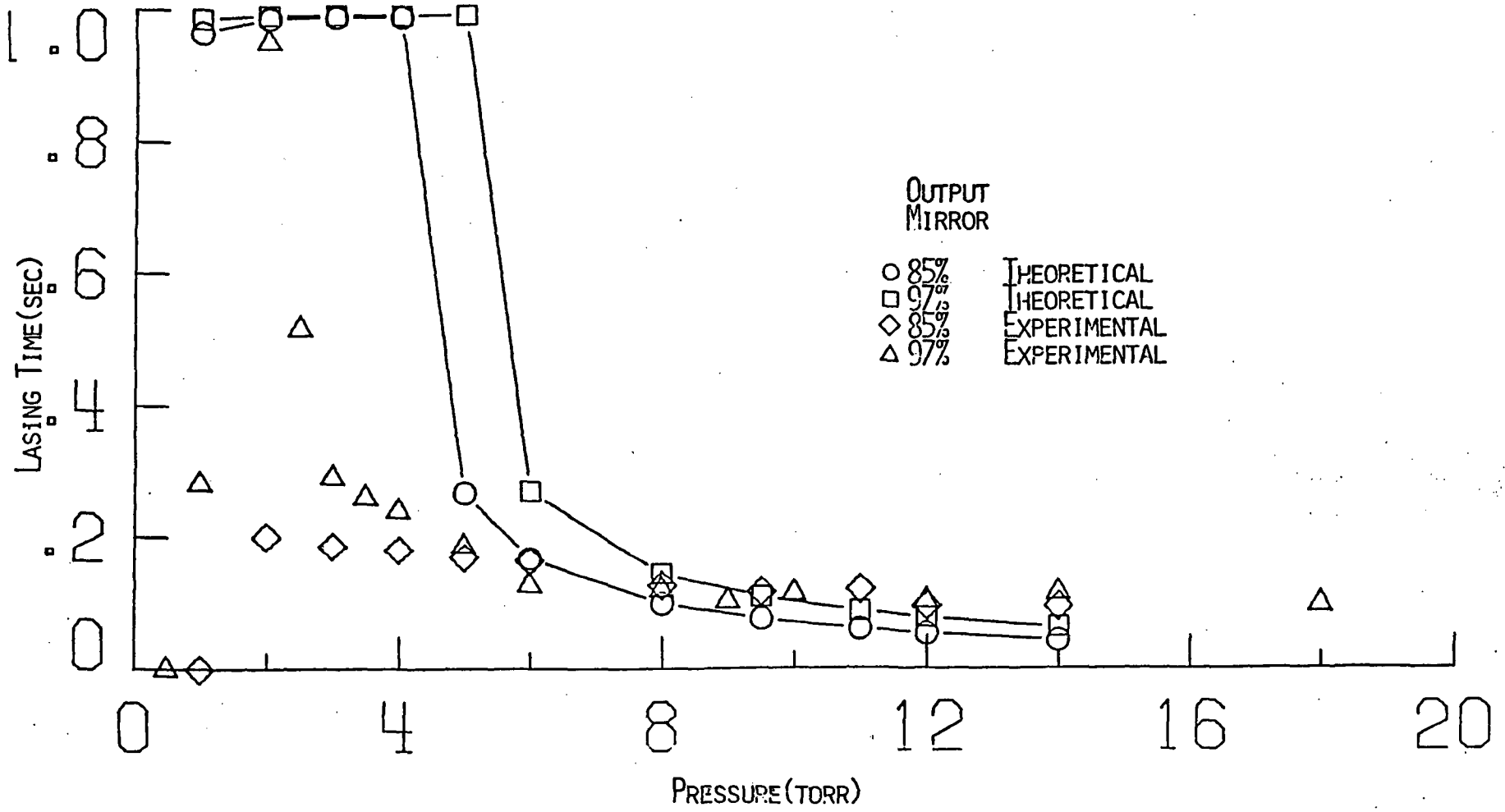
1.0
.8
.6
.4
.2
0
LASING TIME(SEC)
0
4
8
12
16
20
PRESSURE(TORR)
OUTPUT MIRROR
85% THEORETICAL
97% THEORETICAL
85% EXPERIMENTAL
97% EXPERIMENTAL

FIGURE 3.

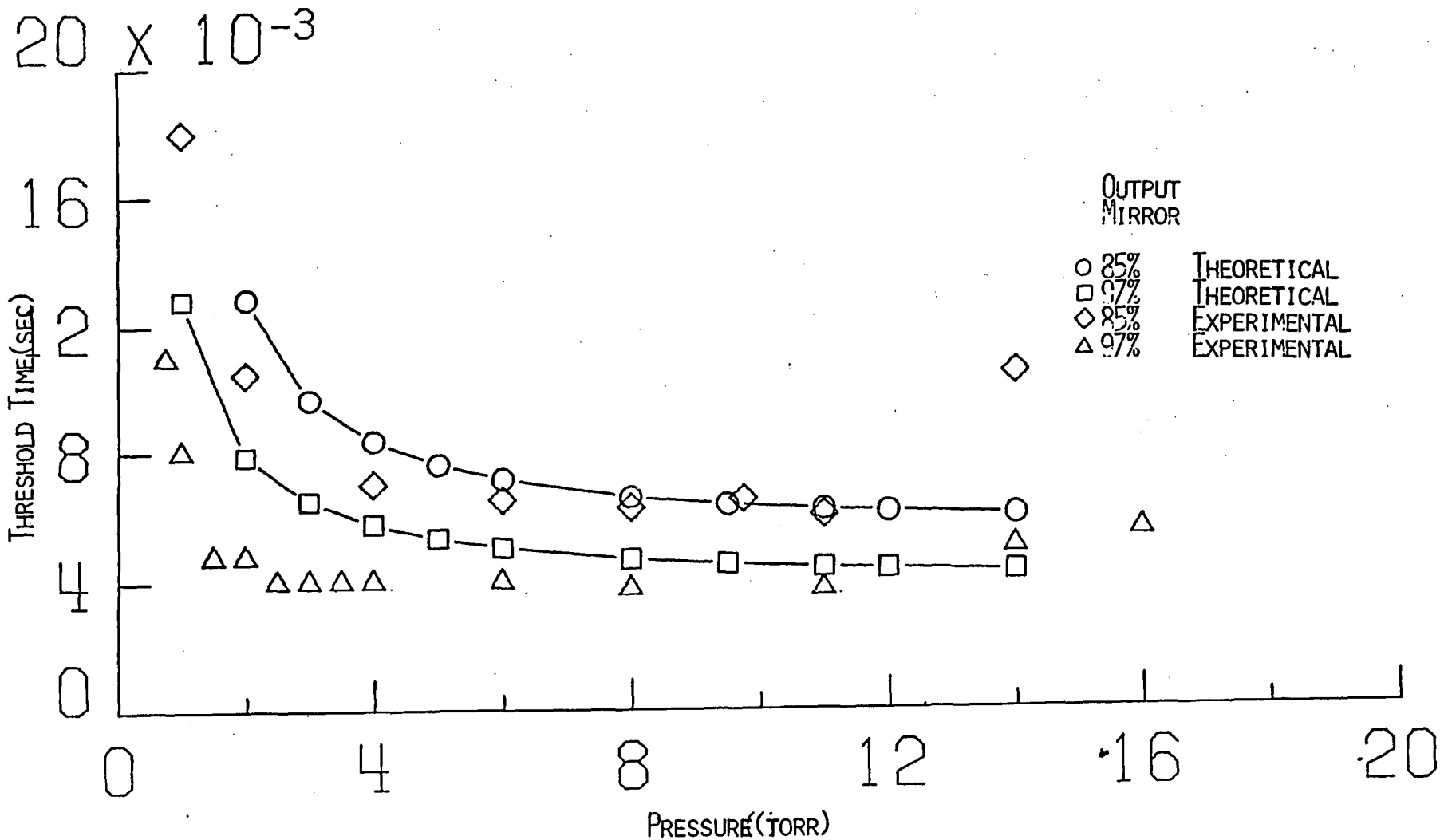
20 X 10⁻³
16
12
8
4
0
THRESHOLD TIME(SEC)
0
4
8
12
16
20
PRESSURE(TORR)
OUTPUT MIRROR
85% THEORETICAL
97% THEORETICAL
85% EXPERIMENTAL
97% EXPERIMENTAL

FIGURE 4.

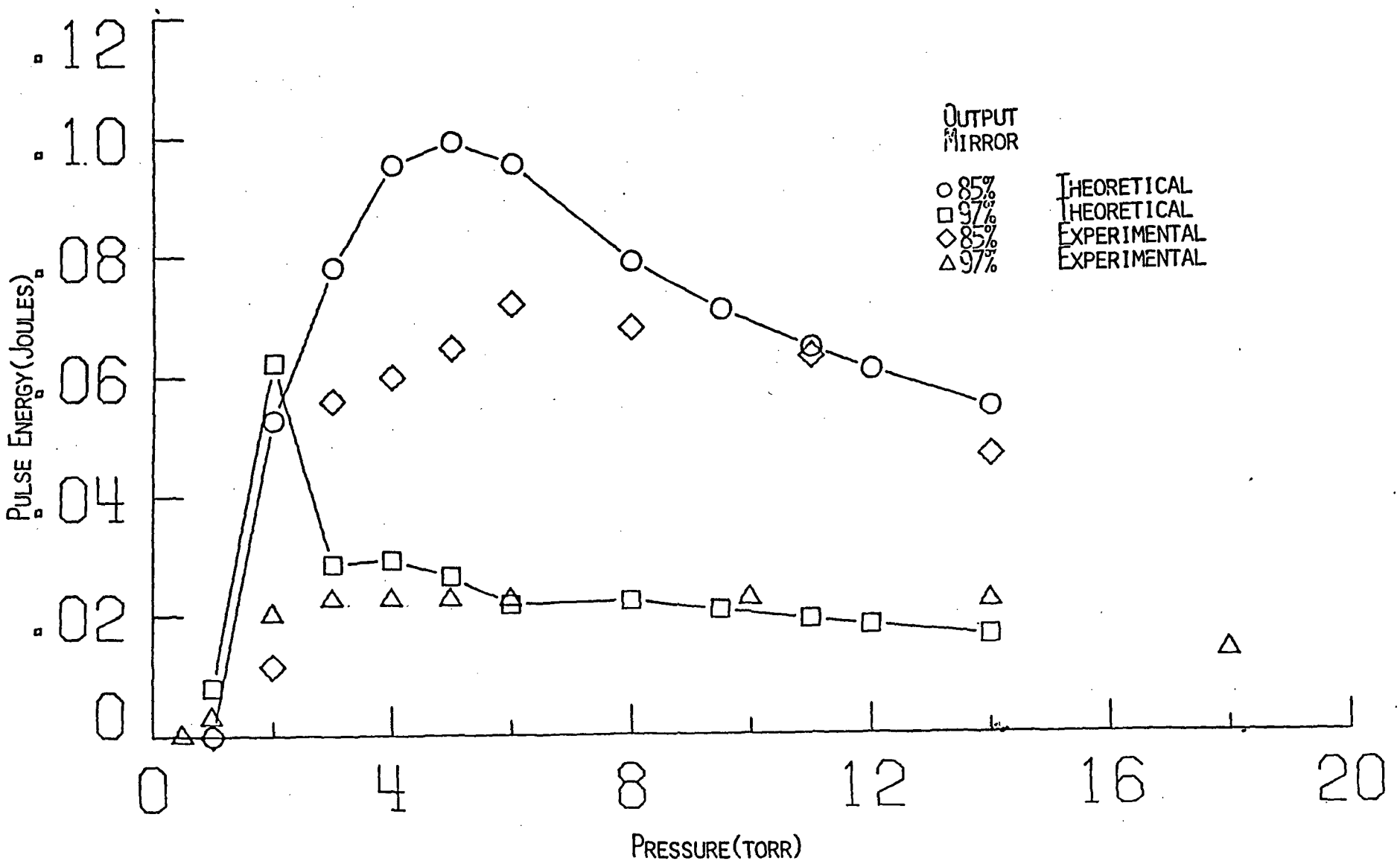
.12
.10
.08
.06
.04
.02
0
PULSE ENERGY (JOULES)
0
4
8
12
16
20
PRESSURE (TORR)
OUTPUT MIRROR
85% THEORETICAL
97% THEORETICAL
85% EXPERIMENTAL
97% EXPERIMENTAL

FIGURE 5.

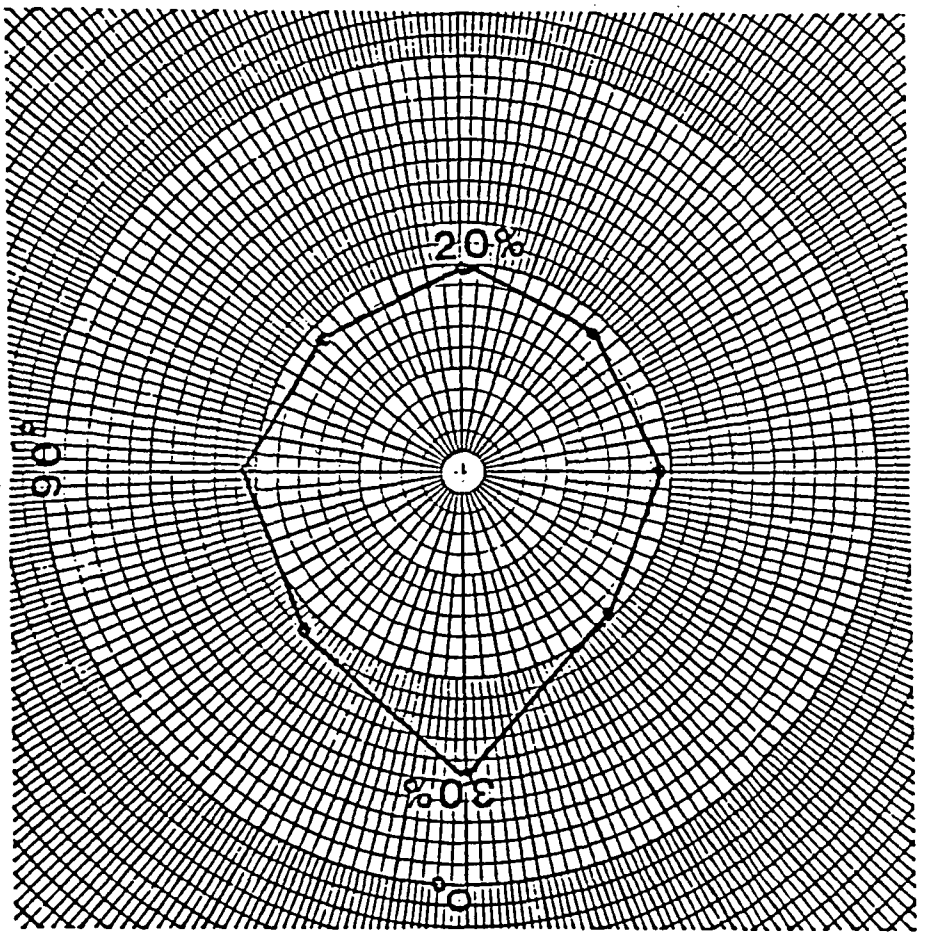

FIGURE 6.

Radial distribution of pumping light intensity.

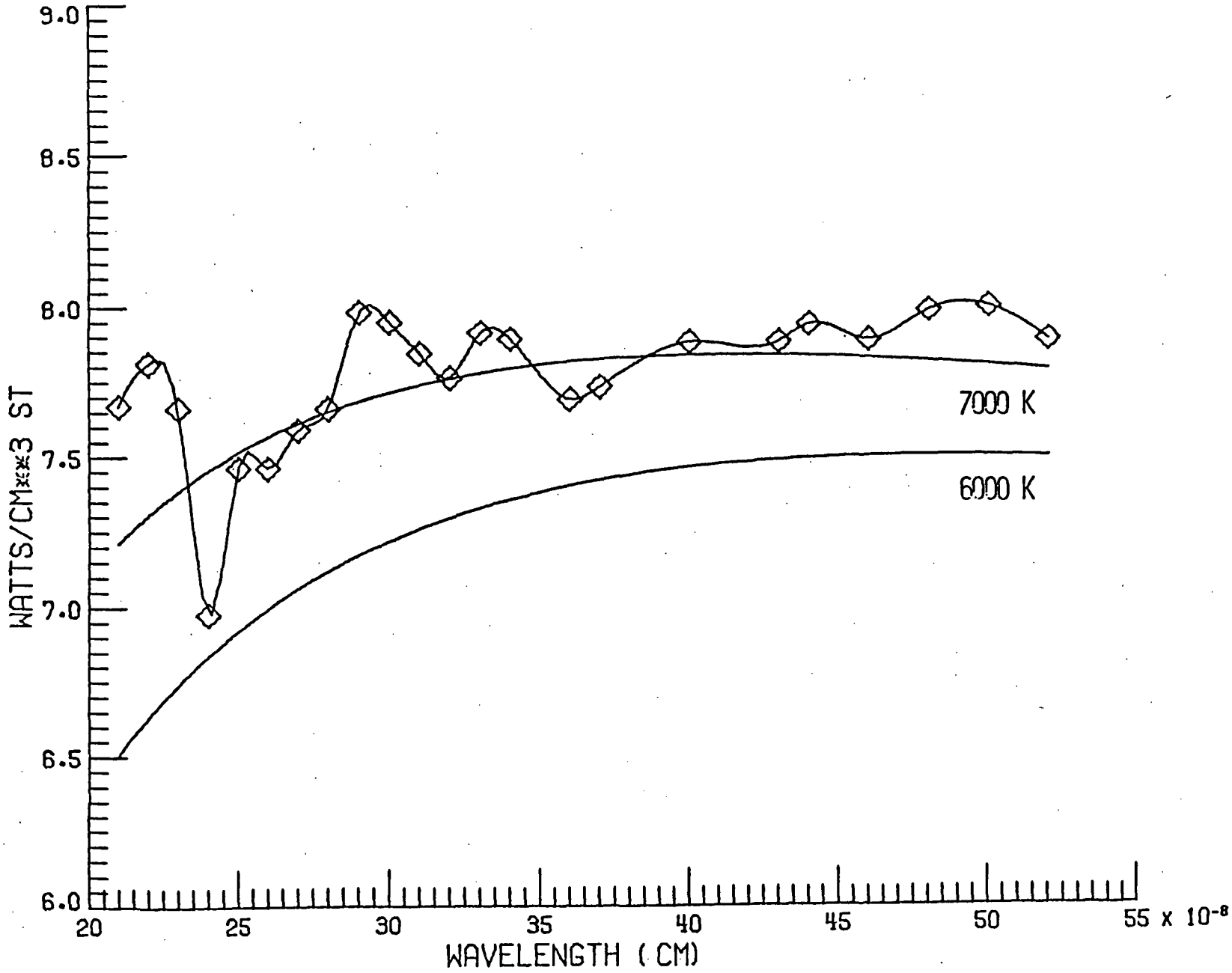
9.0
8.5
8.0
7.5
7.0
6.5
6.0
WATTS/CM**3 ST
7000 K
6000 K
20
25
30
35
40
45
50
55 x 10⁻⁸
WAVELENGTH (CM)

FIGURE 7.

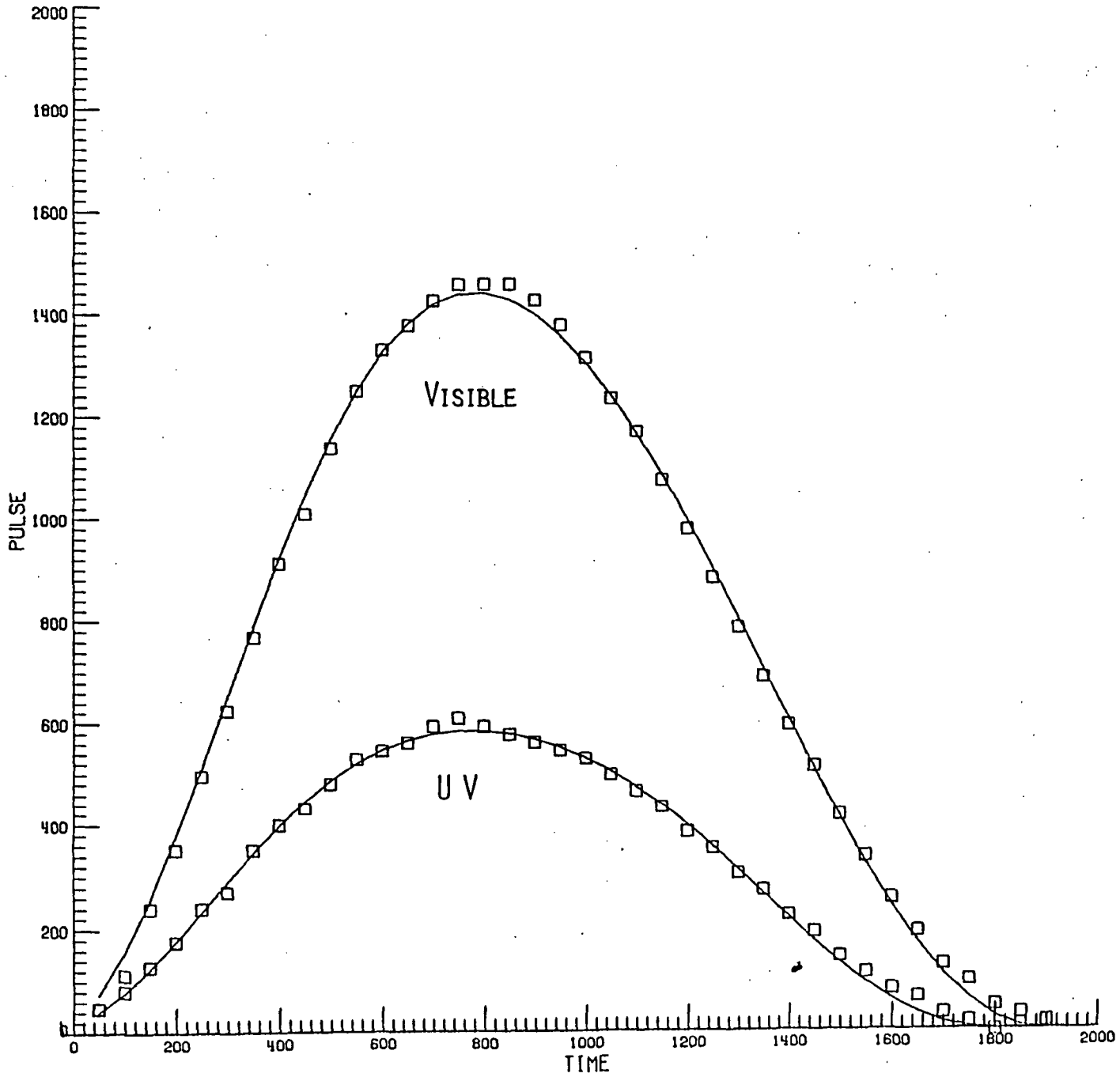
2000
1800
1600
1400
1200
1000
800
600
400
200
0
PULSE
VISIBLE
UV
0
200
400
600
800
1000
1200
1400
1600
1800
2000
TIME

FIGURE 8.

IV. Parametric Studies of Dye Laser Amplifier by Tamarack Solar Simulator

A. Introduction

Since 1980, studies of solar-pumped laser have been reported eleswhere. [1-5] In paricular, laser gain media for direct solar-pumped laser have been investigated considerably [6,7] and organic dyes have been recently considered as active media in solar pumped laser. [8] Figure 1 shows the solar spectrum with air mass zero, absorption and emission spectrum of rhodamine 6G dye. The solar spectrum indicates that 20% of solar energy can be utilized for dye laser pumping because the absorption band of dye, which is suitable for the solar-pumped laser, lies in the 450 to 600nm near the peak of solar spectrum. The quantum efficiency of dye laser is 90% and its tuning range is wide. However, most of researchers have used solid or gas as a lasant, instead of dye, for solar-pumped laser, because most laser dyes have relatively high lasing thresholds. Among laser dyes which are pumped by flashlamp, the lasing threshold of rhodamine 6G dye is lowest and its threshold pump-power density is 50-100KW/cm^2.[9]

Most of solar collectors produce less than threshold pump power density (50-100 KW/cm^2), because the sun is not a point source and concentration limit is imposed by the second law of thermodynamics, i.e., $4x10^4$ solar constant or 5.6KW/cm^2. Thus, it is not sufficient to pump dye laser with power density produced by the typical solar collectors. Even though it is difficult to pump dye laser oscillator directly from the solar radiation due to the high threshold and the limited power density of the solar collector, it is worthwhile to attempt making the solar-pumped dye laser amplifier, because high gain coefficient of dye laser [10], large portion of solar spectrum lying on the aborption band of dye,and the possible optimization of dye laser system such as dye concentration etc.

The purpose of the present experiment is to find out whether the solar-pumped laser amplification is possible or not. Furthermore, it is also to find the optimum condition of laser amplification such as the flow rate of dye solution, dye concentration, triplet quencher concentration, etc. In order to maximize the output energy of the dye laser amplifier, the following factors are considered: the system designation for the effective coupling between solar simulator and laser amplifier, shape design of transverse-flowing amplifier cell to increase repetition rate of laser pulse, long pulse performance, reduction of thermal effect and triplet absorption, [11] etc.

Amplification characteristics of dye laser amplifier have been reported by many authors. [10, 12, 13] Most of these studies were directed toward very short laser pulses, and the pumping power for the amplifier was very stronger than 25 KW/cm^2. On the contrary to such conventional laser amplifier, the solar- pumped laser amplifier cannot be pumped strongly because the available geometrical solar concentration is limited to 40,000 (5.6 Kw/cm^2) constants by the law of thermodynamics. The solar simulator which is used in this experiment produces 10,000 solar constant (or 1.4 KW/cm^2) and pump weakly a laser amplifier. Therefore, it is necessary to study the characteristics of the amplifier system with a weak pump power. For the cw pumping source of the dye laser amplifier, Tamarack solar simulator located at NASA Langley Research Center is used. The optical radiation of the solar simulator is produced by a DC arc discharge across an 8mm gap, which is stabilized by flowing xenon of with pressure of 1,030kPa (10.2atm). As shown in fiugre 2, the light beam emitted from the solar simulator are reflected by a high quality elliptical-reflector (whose aluminum surface is coated by MgF_2 to prevent surface oxidation and abrasion.) before passing through a chopper, and the collector concentrate the beam into a dye laser amplifier. The spectral radiance of the solar simulator corresponds to 6000^oK blackbody radiation. [5]

The maximum electrical input power is 40KW and the optical radiative output is 4KW.[2] The light beam leaving the solar simulator is collected by a 13^{o} cone (7075 aluminum alloy) whose interior surface is polished and coated with MgF_2. Figure 2 shows an experimental set-up of dye laser amplifier system consisting of dye laser oscillator which subsequently injects the periodic laser pulses to the amplifier, and the dye laser amplifier which is continuously pumped by Tamarack solar simulator. The dye laser oscillator is pumped by a flashlamp in this experiment. The dye solution was prepared with a 3:7 mixture of methanol and deionized water and had (rhodamine 6G) dye concentration of $5x10^{-4}$ mol/l. The optical cavity is composed of one full reflector with a flat HR surface, and one output coupler of 2% transmission with a radius of curvature 2m. Figure 3 shows dye laser output as function of input energy. The pulse width of laser output was about 1 us (FWHM).

In designing a laser amplifier cell the following factors were considered. Firstly, the lasing threshold of dye is very short due to the triplet absorption, but the lasing threshold can be extended to 500 us with triplet quencher COT (C_8H_8) [15]. Therefore, the fresh dye solution must be maintained in the dye cell during 500 us in order to have the constant amplification of laser by the pumping light. Secondly, the geometrical dimension of arc image formed along the focal line of the conical collector. When the aperture diameter of the conical collector is 9.6 cm as shown in figure 4, the incident light intensity (FWHM) along the optical axis is 3.27 cm and the light intensity (FWHM) transverse to the optical axis is 4.73 cm. Considering these two factors, the dimension of dye laser amplfier cell becomes 3 mm (height) x3 cm (length) x 2 mm (width). In order to maintain fresh dye solution during the maximum lasing time 500 us, dye flow rate in the cell must be greater than 4 gal/min. There are two ways to circulate dye solution through the amplifier

cell for this purpose. One is a longitudinal flow along the optical axis and another is a transverse flow. In order to maintain dye flow rate 4 gal/min through the amplifier cell, minimum flow speed is 60 m/sec with the longitudinal flow made, and 4 m/sec with the transverse flow mode. In the longitudinal flow, there are many physical limitations such as viscosity etc., because dye solution must pass through the narrow cross-section with a flow speed of 60 m/s. On the contrary, dye soution passes through the wide cross section of cell with a slower flow speed of 4 m/s in the transverse flow. Figure 5 shows a laser amplifier cell with the transverse flow. In order to make dye uniformly flow through the entire section of cell without any turbulance, straighteners, which are made of stainless steel sheets, are inserted as shown in figure 5.

B. Dye Laser Oscillator-Amplifier System.

Figure 6 shows a block diagram of dye laser oscillator and amplifier system used in this experiment. The dye laser oscillator unit is made of dye cell, laser mirrors, flashlamp (ILC Technology Model 7L4) which has 7 mm inner diameter and 101.6 mm are length, and the elliptical reflector. Figure 7 shows the pumping light (upper) and the laser output (lower) as a function of time. The pulse width of the laser light (FWHM) is 1 us. The dye laser amplifier unit consists of dye cell for amplifier, conical collector, dye circulator and coolong unit. An attenuator and beam splitter are located between oscillator and amplifier. Laser input energy to amplifier and output energy from amplifier are monitored through fiber optics cable whose diameter is 5mm. Using a beam splitter, a small fraction of laser output from oscillator is extracted to monitor the input energy to amplifier, and 1/1000 of laser ouput from oscillator actually passes through the amplifier. A photodiode (EG&G

Model SGD 040 D) is used for the detection of the laser input signal and a photomultiplier tube (Amperex Model 2018B) for laser output signal from amplifier. Input and output pulses from the amplifier were recorded photographically from the dual-beam oscilloscope (Tektronix 556) and C-19 camera. As shown in figure 6, photodiodes PD1 and PD3 monitor light from flashlamp which pumps oscillator, and light from solar simulator which pumps amplifier respectively. Consequently, injection time of laser pulse into amplifier is calculated.

C. Fluorescence Measurement.

Figure 8 shows a schematic diagram of monitoring the light intensity of rhodamine 6G fluorescence, which is emitted from the amplifier cell, with a photomultiplier tube. In order to estimate the fluorescence signal to noise ratio, the fluorescence light emitted from the center of the dye cell is focused through lens L before entering into a P.M. tube. A flat mirror which is located 45^{o} relative to amplifier cell diverts fluorescent light into a P.M. tube. A fiber optics cable transmits the fluorescence light into the detector of the photomultiplier tube whose signal is monitored by an oscilloscope. Before rhodamine 6G dye dissolves into a methanol solvent, the noise level, which is associated with the fluorescence light signal in the methanol solvent, is determined. Next the fluorescence light signal from rhodamine 6G dye solution is measured. From the results of the fluorescence light, the following relations are determined:

i The intensity of fluorescence light which is proportional to concentration of the excited singlet-singlet state, is used for the comparison of amplifier output.

ii Since the triplet absorption becomes considerably large after the fluorescence light reaches peak, amplifier gain becomes negative.

Using the estimated time to reach fluorescence peak, the optimum injection time of input energy to the amplifier can be determined.

iii By measuring these time variation of fluorescence peak, its peak duration, and the optimum dye concentration can be determined.

D. Amplifier gain measurement.

Figure 9 shows oscillograms of both input and output signals before and after the amplifier is on. From these oscillograms, the intensity of input energy can be calculated by normalizing the detector response of the input energy. Then the ratio of the laser output with the amplifier "on" to the calculated input above gives amplifier gain and exponential gain coefficient.

E. Amplifier Gain Measurement as a Function of the Injection Time.

In order to measure amplifier gain as a function of the injection time when pumped with the laser output of the oscillator, the lasing time of oscillator is adjusted with a time delay generator. As shown in figure 6, the light signal generated when pumping amplifier with a solar simulator is transmitted to photodiode PD3 via a fiber cable and subsequently the light from the photodiode triggers the time delay generator. After preset delay up to 100 usec, the flashlamp of the oscillaotr could be energized.. As a result, amplifier gain is measured as a function of time. Time delay of light signal between solar simulator and flashlamp is measured with Nicolet digital oscilloscope (Model 2090). The time behavior of amplifier gain is measured with or without a triplet quencher COT (C_8H_8) in rhodamine 6G dye solution. As mentioned in the section of fluoresecene measurement, the amplification gain is sharply reduced without the triplet quencher, but the steady amplifier gain is maintained for a relatively long time in the presence of the triplet quencher. By measuring the reduction rate of amplifier gain, the effect of COT is estimated.

F. References

1. Laser Focus, "First Solar-Pumped Gas Laser is Operated at NASA-Langley", 17, NO3, 16 (1981).

2. Ja H. Lee, W.R. Weaver, "A Solar Simulator-Pumped Atomic Iodine Laser", Appl. Phys. Lett. 39, 137 (1981).

3. H. Arashi, Y. Oka, N. Sasahara, A. Kaimai, M. Ishigame, "A Solar-Pumped cw 18W Nd: YAG Laser", Jap. J. Appl. Phys. 23, 1051 (1984).

4. A.L. Gogler, I.I. Klimovsky, "Lasers Pumped by Solar Radiation", Sov. J. Quantum Electron. 14, 164 (1984).

5. J.W. Wilson, Y. Lee, W.R. Weaver, D.H. Humes, Ja H. Lee, "Threshold Kinetics of a Solar-Simulator-Pumped Iodine Laser", NASA TP-2241 (1984).

6. J.W. Wilson, "Solar-Pumped Gas Laser Development", AIAA 19th Aerospace Sciences Meeting, Paper No. 18-0098, St. Louis, Missouri (1981).

7. A.L. Golger, I.I. Klimovsky, "Solar-Pumped Lasers", Int. Conf. Laser-83, Tech. dig. p686, San Francisco, California (1983).

8. M.D. Williams, "Intensity and Absorbed-Power Distribution in a Cylinderical Solar-Pumped Dye Laser", NASA TP-2321 (1984).

9. F.P. Schafer, Dye Lasers in Topics in Applied Physics, Springer-Verlag, Berlin (1977).

10. B.G. Huth, "Direct Gain Measurement of an Organic Dye Amplifier", Appl. Phys. Lett. 16, 185 (1970).

11. H.W. Friedman, R.G. Morton, "Transverve Flow Flashlamp Pumped Dye Laser", Appl. Opts. 15 1494 (1976).

12. U. Ganiel, A. Hardy, G. Neumann, D. Treves, "Amplified Spontaneous Emission and Signal Amplification in Dye-Laser Systems", IEEE. J. Quantum Electron. QE-11, 881 (1975).

13. K. Namba, J. Ida, "Copper Vapor Laser Pumped Dye Amplifier of a CW Dye Laser", J. Appl. Phys. 23, 1330 (1984).

14. I.H. Hwang, K.S. Han, "Solar-Pumped Iodine Laser Amplifier", Technical Digest in International Congress of Laser Application and Electro-Optics (ICALEO '84) Cong., Boston, Massachusetts (1984).

15. R. Pappalardo, H. Samelson, A. Lempicki, "Long-Pulse Laser Emission from Rhodamine 6G", IEEE J. Quantum Electron, QE-6, 716 (1970).

G. List of figures

Fig. 1 Absorption and emission spectra of rhodamine 6G as compared with air mass zero solar spectrum.

Fig. 2 Schematic diagram of experimental setup for solar-pumped dye laser amplifier.

Fig. 3 Output energy of rhodamine 6G laser as a function of electrical input energy.

Fig. 4 Distribution of solar simulator irradiance along the center line of 9.6cm aperture cone.

Fig. 5 A cross-sectional view of dye laser amplifier head and side view of straightner structure.

Fig. 6 Schematic diagram of experimental setup for gain measurement: A: aperture, BS: beam splitter, FO: fiber optics cable, ND: neutral density filter, PD: photodiode, PM: photomultiplier tube, S: shutter.

Fig. 7 Oscillograms of a pumping light pulse (upper beam) and rhodamine 6G laser pulse (lower beam).

Fig. 8 Schematic diagram of experimental setup for fluorescence measurement.

Fig. 9 Typical oscilloscope trace of the amplifier input and output

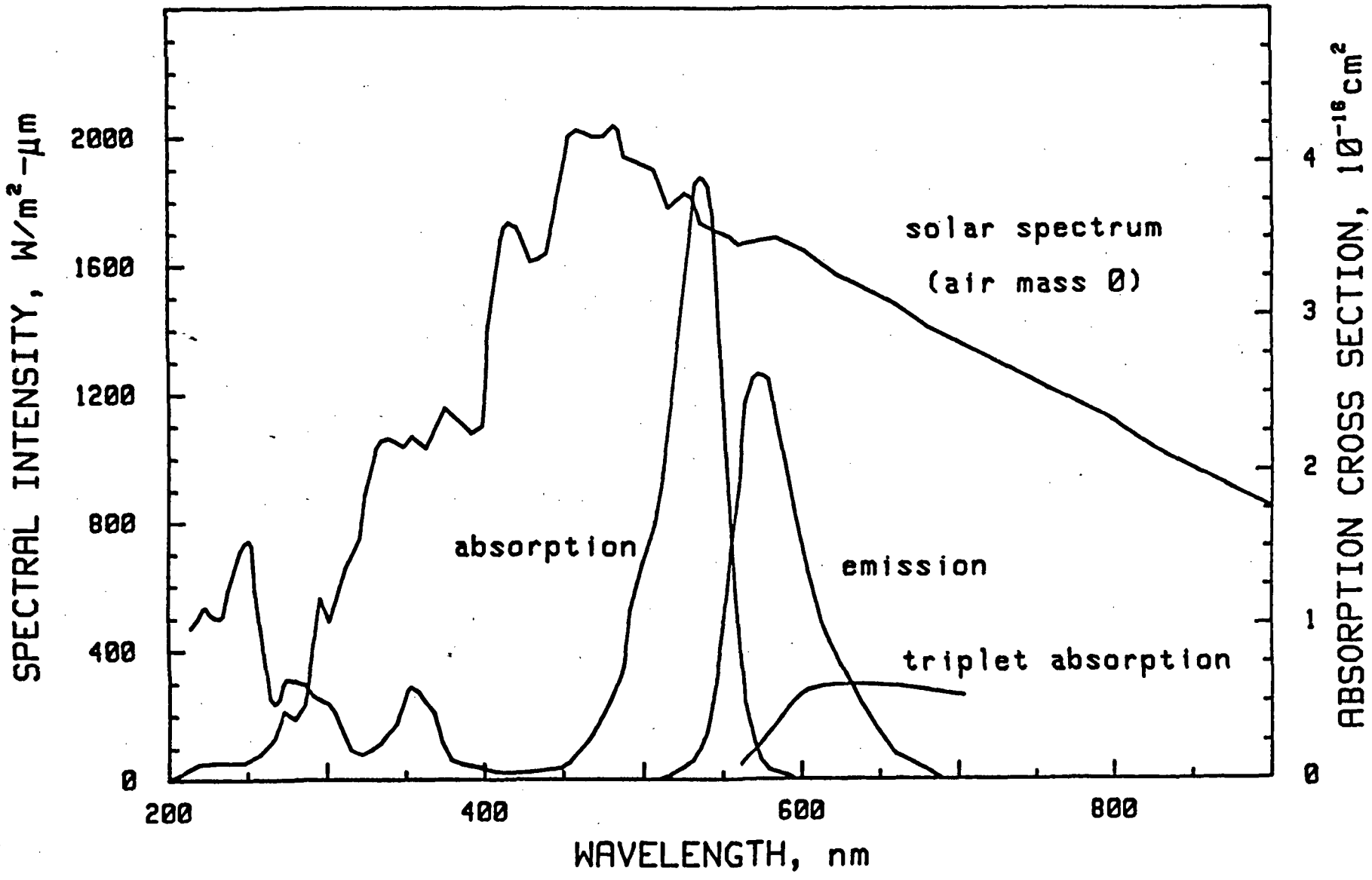

Fig. 1 Absorption and emission spectra of rhodamine 6G as compared with air mass zero solar spectrum.

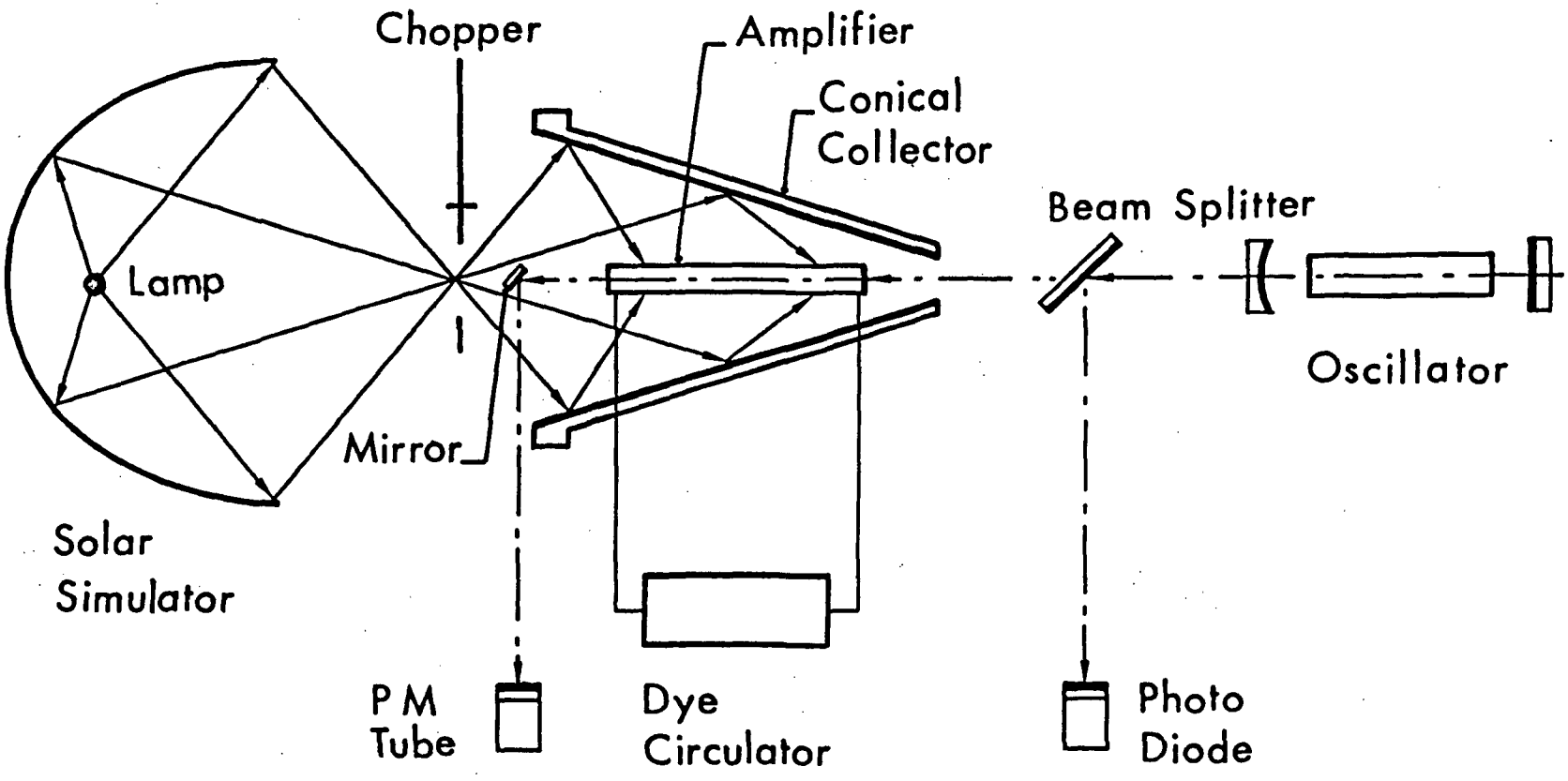

Fig. 2 Schematic diagram of experimental setup for solar-pumped dye laser amplifier.

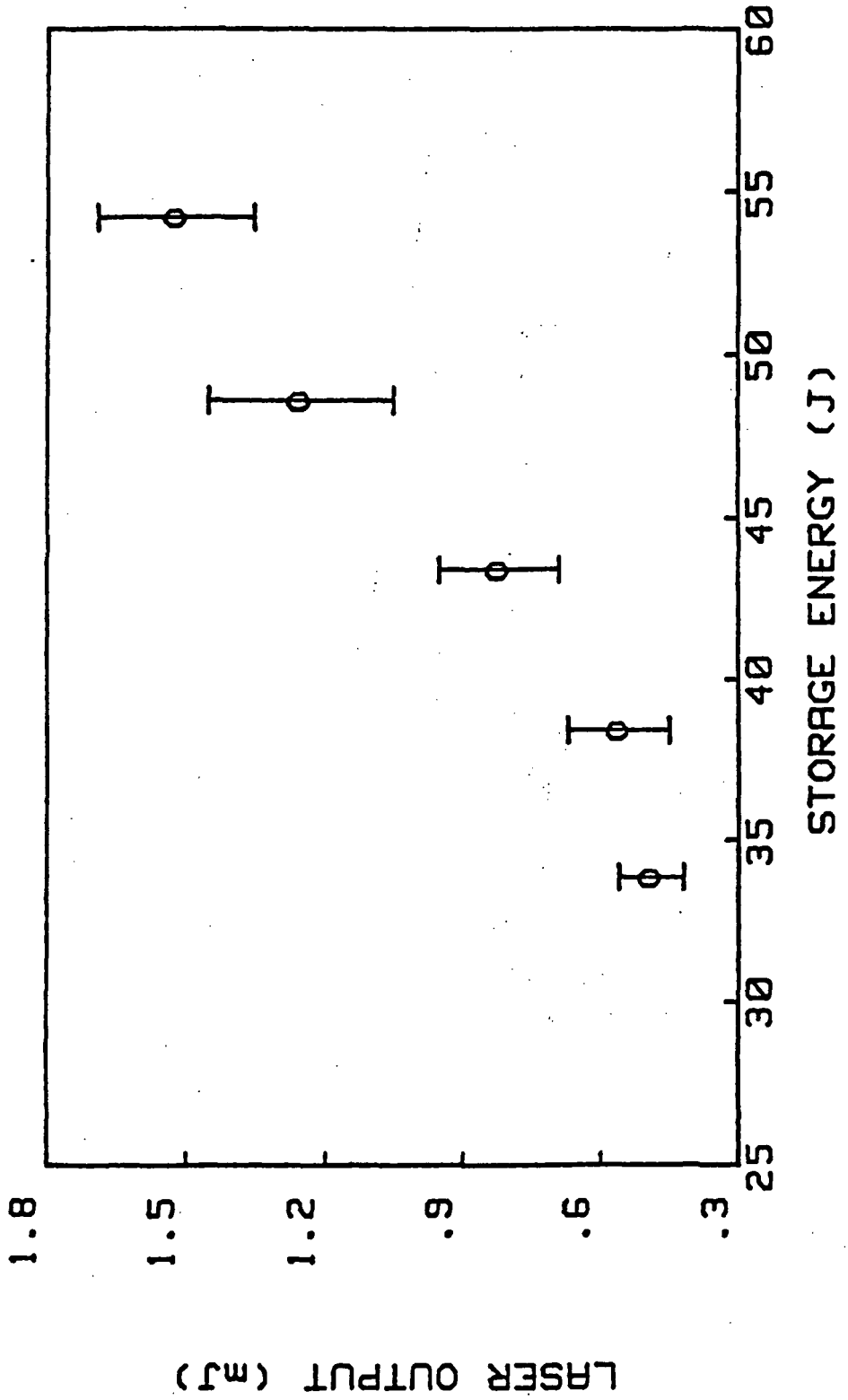

Fig. 3 Output energy of rhodamine 6G laser as a function of electrical input energy.

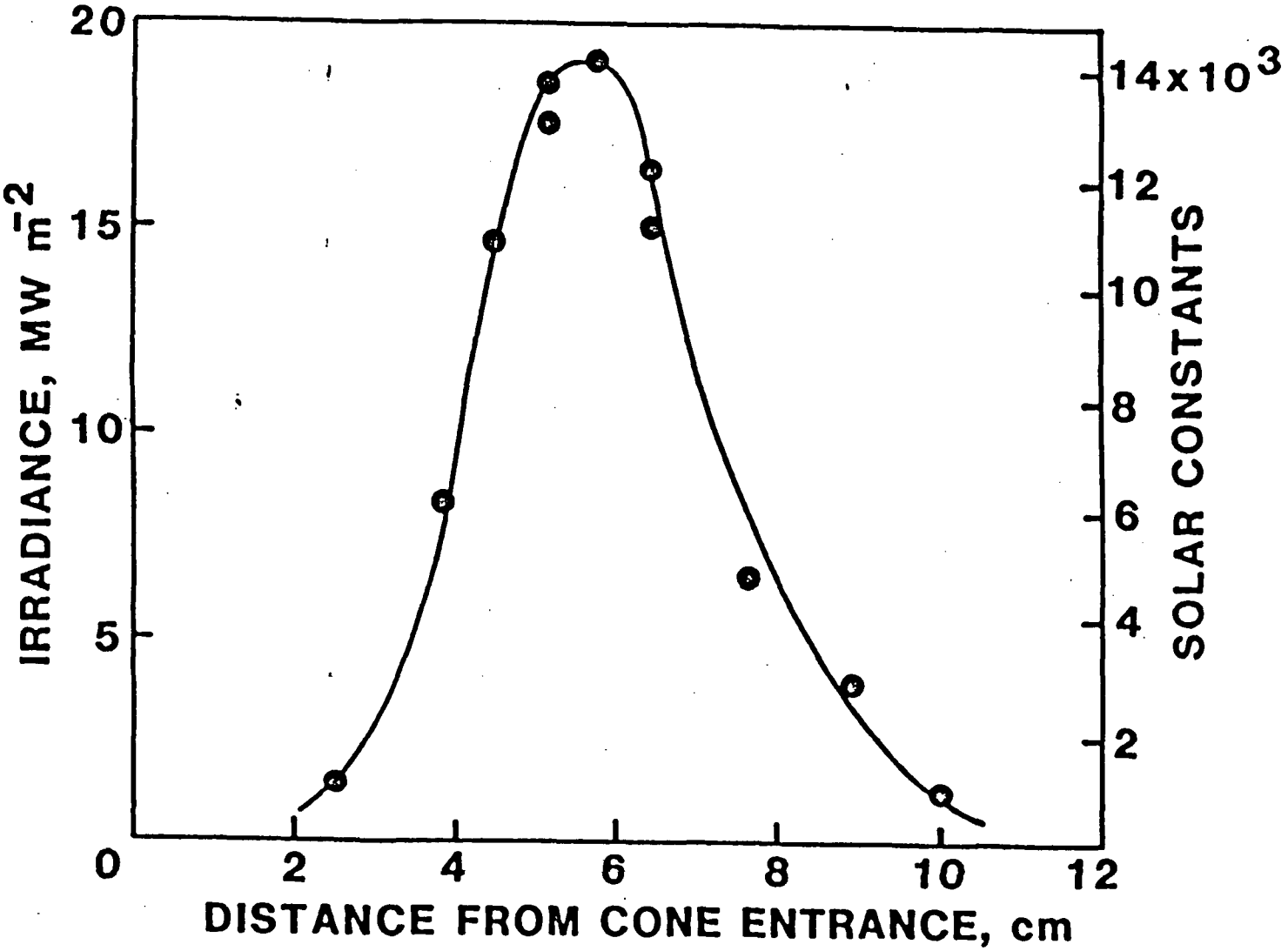

Fig. 4 Distribution of solar simulator irradiance along the center line of 9.6cm aperture cone.

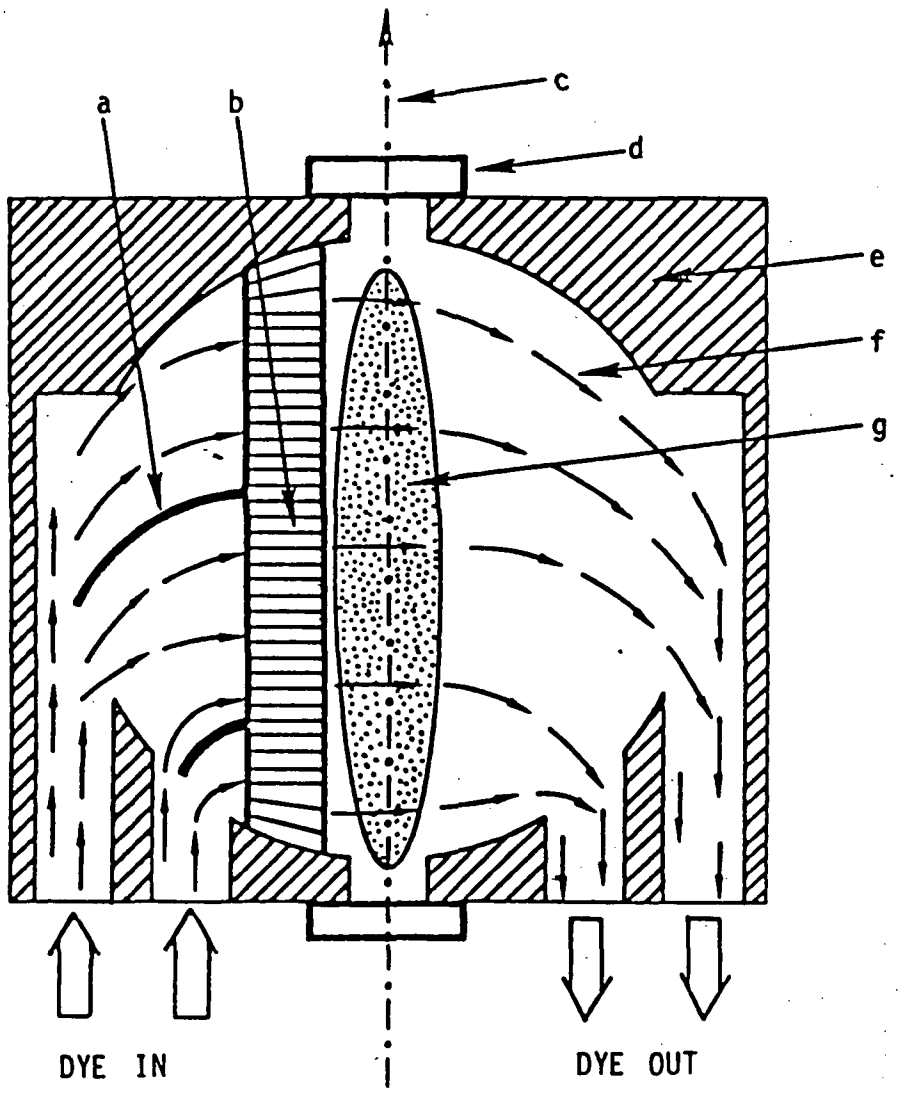

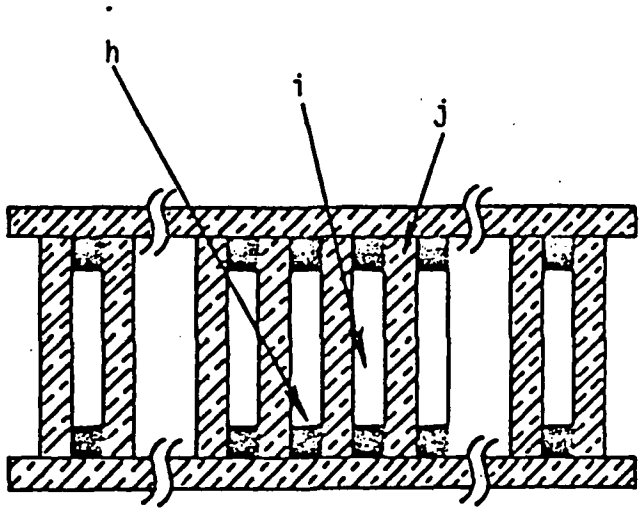

a - Diffraction plate
b - Straightner
c - Optical axis
d - window
e - Teflon body
f - Dye flow
g - Exposed region
h - Dye flow path
i - SS spacer (0.15mm)
j - SS plate (0.12mm)

Fig. 5 A cross-sectional view of dye laser amplifier head and side view of straightner structure.

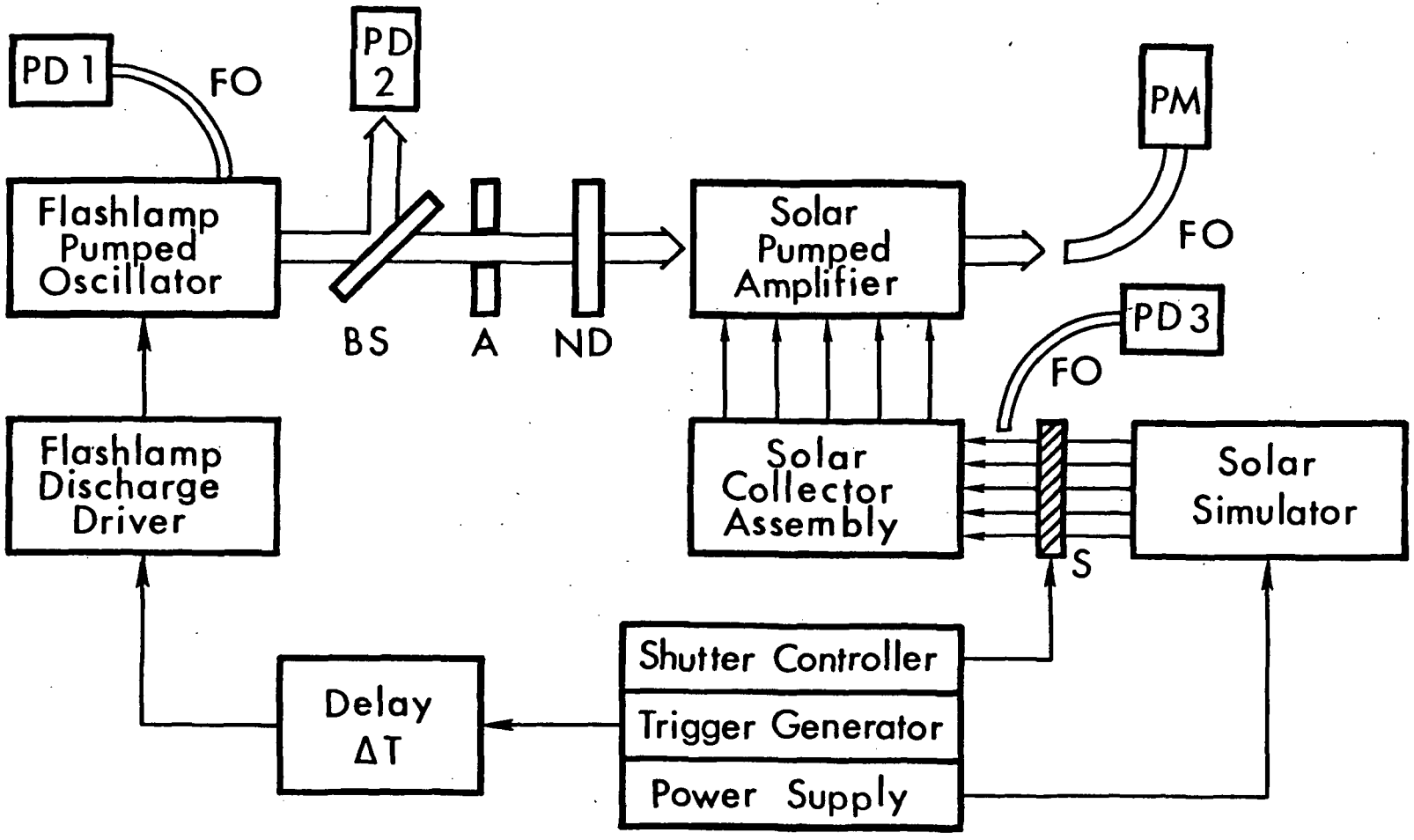

Fig. 6 Schematic diagram of experimental setup for gain measurement: A: aperture, BS: beam splitter, FO: fiber optics cable, ND: neutral density filter, PD: photodiode, PM: photomultiplier tube, S: shutter.

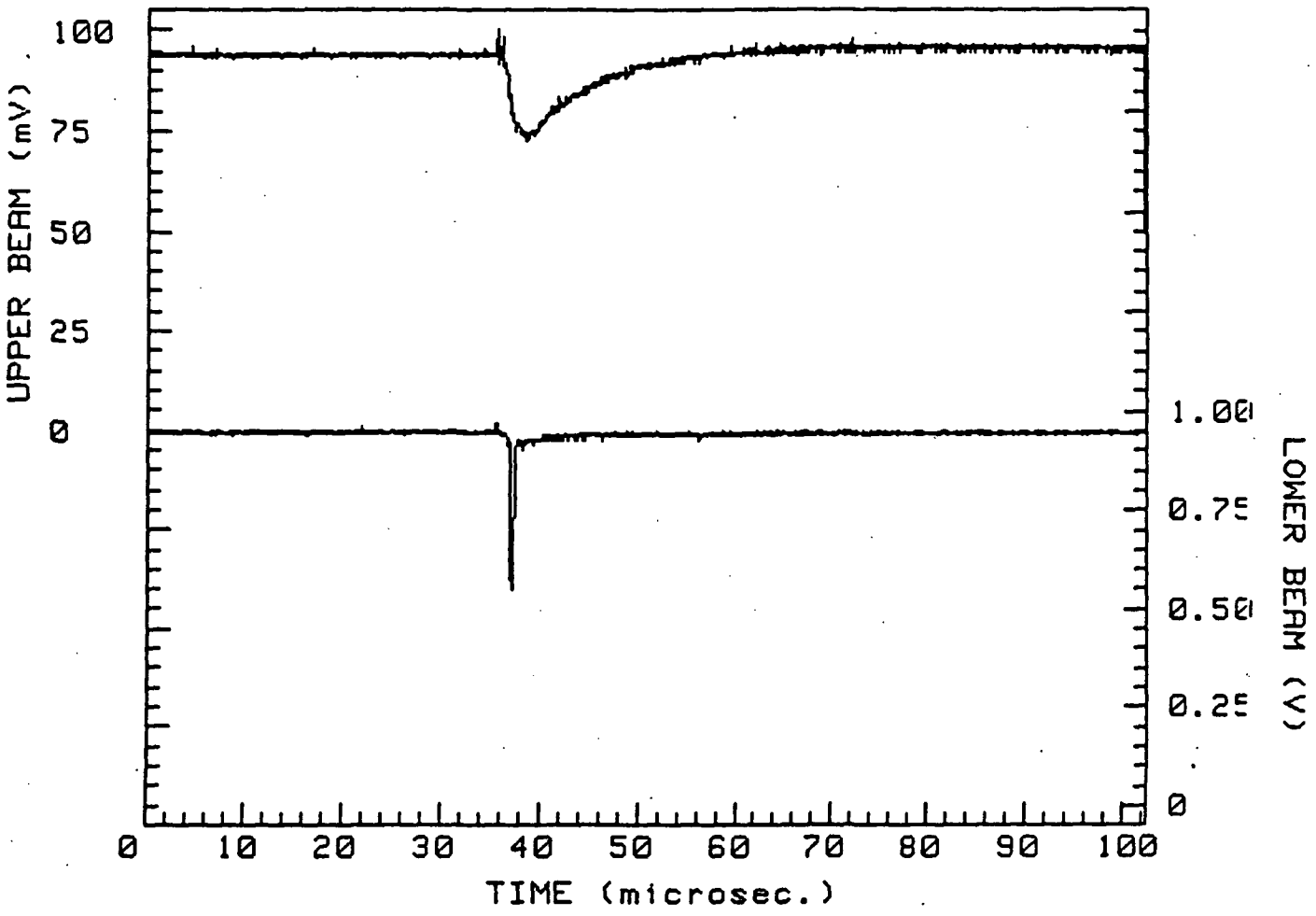

Fig. 7 Oscillograms of a pumping light pulse (upper beam) and rhodamine 6G laser pulse (lower beam).

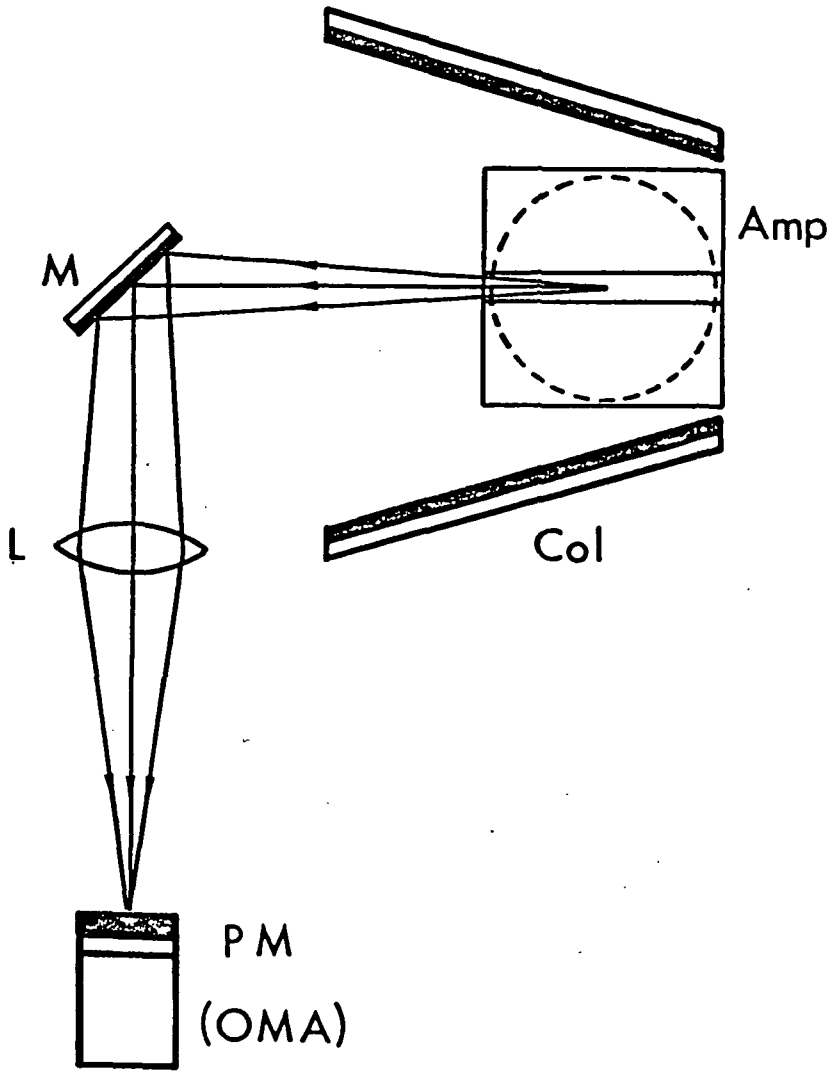

Fig. 8 Schematic diagram of experimental setup for fluorescence measurement.

Fig. 9 Typical oscilloscope trace of the amplifier input and output.